

CONTENTS

ABSTRACT	V
EXECUTIVE SUMMARY	VII
1 INTRODUCTION	1-1
Background and objectives	1-1
Nomenclature for washer configurations	1-4
Analysis and design questions	1-5
Organization of the report.....	1-6
2 PROPOSED ANALYSIS PROCEDURE	2-1
3 CYCLIC FORCE-DISPLACEMENT BEHAVIOR OF WASHER STACKS	3-1
4 SHAKE TABLE EXPERIMENTS	4-1
Test setup	4-1
Instrumentation	4-1
Determination of CVT inertia properties.....	4-4
Washer stack installation.....	4-5
Test configurations and protocol.....	4-5
Correlating measured forces and accelerations.....	4-6
5 NONLINEAR MODELING AND ANALYSIS	5-1
From stack force-displacement to system moment-rotation.....	5-1
Modeling moment-rotation hysteresis.....	5-2
Summary of nonlinear dynamic model	5-3
Analysis results	5-5
6 EQUIVALENT LINEAR MODELING.....	6-1
Identifying equivalent frequency and damping ratio from measurements.....	6-1
Graphical determination of equivalent stiffness and damping ratio	6-1
Response-spectrum interpretation.....	6-4
7 SUMMARY AND CONCLUDING REMARKS	7-1
Recommended analysis and design procedure	Error! Bookmark not defined.
Outstanding research questions	7-1
8 REFERENCES	8-1

LIST OF FIGURES

Figure 1-1 Belleville washer shape, dimensions and stack consisting of series-parallel arrangement.....	1-1
Figure 1-2 Force-displacement response of a single washer as a function of h/t (source [7]).....	1-2
Figure 1-3 Capacitive voltage transformer (CVT) provided by Seattle City Light and used in shake table experiments described in Chapter 4	1-5
Figure 3-1 Washer stack force-displacement response measurement by <i>compressing the stack directly</i> in the materials testing machine; force-displacement response exhibits unexpected changes in slope	3-1
Figure 3-2 Washer stack force-displacement response measurement by <i>compressing the stack through a loading frame with guiding rod</i> ; this is closer to how the washers are mounted under the equipment, and the force-displacement response is clean.....	3-2
Figure 3-3 Measured force-displacement curves for two configurations. The legend MTS denotes measurement from the materials testing machine through the frame with guiding rod. The other curves are in situ measurements from the shake table at different preload levels. The in situ measurements follow the testing machine results closely, confirming that the washer stack response can be characterized fully using simply a materials testing machine.....	3-2
Figure 3-4 Measured force-displacement curves for two configurations with the K1750-J-057 washers. They have a softening behavior because of their larger h/t ratio (cf. Figure 1-2)	3-3
Figure 4-1 CVT mounted on shake table	4-1
Figure 4-2 Instrumentation details	4-2
Figure 4-3 Details of Load Washer Alternate (LWA) and preloading process	4-3
Figure 4-4 CVT mounted on springs to estimate mass moment of inertia indirectly from measured frequency.....	4-4
Figure 4-5 Acceleration measured when CVT is mounted on springs and the resulting frequency fit, and process to compute CVT mass moment of inertia from measured frequency; the dimension b is 6.375in in the X direction and 9.25in in the Y direction.	4-4
Figure 4-6 5%-damped test response spectra of applied CERL motion compared with required response spectrum.....	4-5
Figure 4-7 Free body diagram with mid-spool cut.....	4-6
Figure 4-8 Correlation between the independent measurements, Mspool and -I0θ-mxtL, demonstrating consistency for the 2 units of 2U2D configuration under 0.5g CERL motion in the X direction.....	4-7
Figure 4-9 Free body diagrams relating moment measured at the spool with moment estimated using LWAs.....	4-8
Figure 4-10 Free body diagram used to relate insulator base moment to measured accelerations; L_1 is the mid-height of the insulator, $L_1 = \text{in}$; $L_2 =$ the distance from the center of rotation to the center of mass of the insulator, $L_2 = \text{in}$	4-9
Figure 4-11 Correlation between Mspool and MCVT per equation (4-6) demonstrating consistency for the 2 units of 2U2D configuration under 0.5g CERL motion in the X direction.	4-11
Figure 4-12 Measured insulator base moment for the different configurations for 0.5g CERL motion applied in the X direction	4-13
Figure 4-13 Measured insulator base moment for the different configurations for 0.5g CERL motion applied in the Y direction	4-14

Figure 5-1 Process to obtain moment-rotation behavior from washer-stack force displacement behavior	5-1
Figure 5-2 Example of constructing the moment-rotation behavior from the stack force-displacement behavior for 2 units of 2U2D	5-1
Figure 5-3 Parallel decomposition of moment-rotation behavior into elastic and hysteretic components (example shown for 2 units of 2U2D).	5-2
Figure 5-4 Comparison on model and measured moment-rotation behavior when the model is driven by the measured θ_w as input (example shown for 2 units of 2U2D).....	5-3
Figure 5-5 Relative magnitudes of total CVT rotation θ , washer stack deformation θ_w and spool plate deformation θ_p (example shown for 2 units of 2U2D in X direction for 0.5g CERL motion).....	5-4
Figure 5-6 Various response quantities obtained from nonlinear dynamic analysis compared with corresponding measurements for 2 units of 2U2D in X direction for 0.5g CERL motion with 50% preload.....	5-6
Figure 5-7 Various response quantities obtained from nonlinear dynamic analysis compared with corresponding measurements for 2 units of 2U2D in X direction for 0.5g CERL motion with 25% preload.....	5-7
Figure 6-1 Concept of graphically obtaining equivalent stiffness and damping ratio.	6-1
Figure 6-2 Comparison of measurements with linear fit obtained using subspace system identification for 0.5g CERL excitation in the X direction for 2 units of 2U2D configuration.....	6-2

No table of figures entries found.

LIST OF TABLES

Table 1-1 Washers used in this project [22]	1-4
Table 1-2 Nomenclature used for Belleville washer units and stacks	1-4
Table 4-1 Summary of measured response quantities and corresponding instruments	4-2
Table 4-2 Response quantities derived indirectly from measurements.....	4-3
Table 4-3 Summary of CVT inertia properties	4-4
Table 4-4 Summary of configurations tested	4-5
Table 4-5 Summary of CVT inertia properties	4-6
Table 6-1 Summary of findings from experimental measurements and equivalent linear modeling for 0.5g CERL excitation. Damping ratios in parentheses denote those obtained by the procedure in XXX.	6-3

No table of figures entries found.

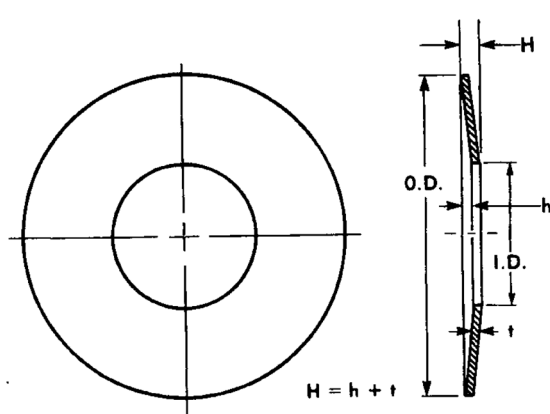
1

INTRODUCTION

Background and objectives

Base isolation and supplemental damping systems are now widely used as seismic protective systems in structures. They represent a design philosophy that seeks to reduce seismic demand on functional structural components, and to minimize if not eliminate damage and permanent deformation even under large earthquakes. This is in contrast to the conventional seismic design philosophy, wherein structural components are designed to be ductile, and undergo permanent deformation without failure. For critical structures and equipment, such as in electrical substations, the approach of reducing seismic demand and permanent deformations is more attractive to ensure continued functioning of such structures and equipment post-earthquake. The concept of frequency modification for substation equipment was recommended as early as 1973 in a report prepared for Bonneville Power Administration (BPA) [1]. Base isolation and supplemental damping systems are being increasingly deployed in substations for seismic protection [2-5].

One approach to modifying frequency and adding damping is using stacks of Belleville washers. Belleville washers, named after Julian Belleville, who patented them in 1867, are circular washers given a taper to form a conical shape (Figure 1-1a). They are also known as a disc springs or conical spring washers, although the term “disc springs” may be more appropriate [6] for the type of dynamic application considered in this report. When a compressive load is applied along the axis, the washer flattens by way of elastic deformation, resulting in spring action [7]. When washers are nested such that the bottom surface of one is placed on the top surface of the next, frictional rubbing between these surfaces results in hysteretic behavior (see Chapter 3), and



(a) Shape and dimension specifications
(source: [7])



(b) Example of a stack with series-parallel arrangement

Figure 1-1
Belleville washer shape, dimensions and stack consisting of series-parallel arrangement

hence energy dissipation. The washers can also be stacked in different ways as illustrated in Figure 1-1 and Table 1-2. Thus the stiffness and dissipation of a stack of Belleville washers can

be tuned. Testing discussed further in Chapter 3 has shown that the force-displacement hysteresis of washer stacks is stable and repeatable. These stacks therefore lend themselves to modeling, and use as engineered frequency modification and energy dissipation devices.

For early analyses of the mechanical behavior of Belleville washers, see [8, 9], considering both single washer and nesting. For a more recent study on the analysis of washer mechanical behavior, see [10] and the references therein. The force-displacement behavior of a single washer is given by [7, 9]

$$F = \frac{E\delta}{(1-\mu^2)Ma^2} \left[(h - \delta) \left(h - \frac{\delta}{2} \right) t + t^3 \right] \quad (1-1)$$

where F and δ are the force in the washer and deflection, E and μ are the Young's modulus and Poisson ratio of the washer material, M is a constant that depends on the ratio of outer to inner diameters (see [7] for a chart), a is the outer radius and h and t are the dimension shown in Figure 1-1. Depending on the h/t ratio, equation (1-1) implies a wide variety force-displacement behaviors as shown in Figure 1-2. As a point of reference, the washers used in the present project are listed in Table 1-1. The K1875-G-086 washer has a h/t ratio of 0.5, which corresponds to almost linear behavior till flattening. The K1750-J-057 washer on the other hand has a h/t ratio of 1.0 resulting in a force-displacement curve that softens significantly before flattening. These behaviors are reflected in the test results in Chapter 3. Specific features of the force-displacement behavior can be exploited¹. An even wider range of behavior has been explored using Belleville-washers made of shape-memory materials [12].

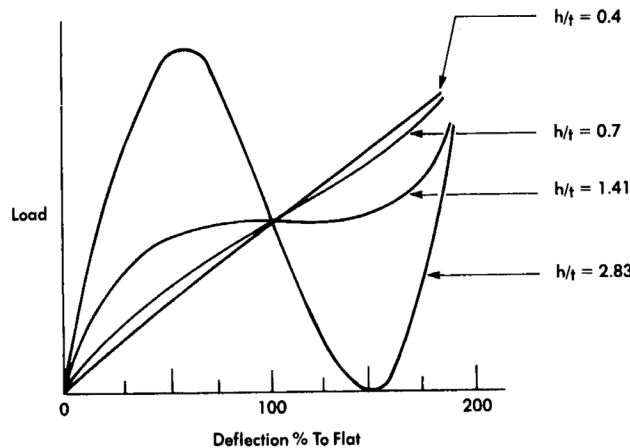


Figure 1-2
Force-displacement response of a single washer as a function of h/t (source [7])

Belleville washers have been used in a number of industries for vibration isolation/absorption applications (see for example [13]). This includes seismic protective systems. Used of large

¹ for example, by preloading washers of h/t of about 1.5 have nearly zero stiffness at flattening; so by preloading such washers to flattening and providing spacing to deformed beyond flattening, an isolation system with nearly zero frequency can be achieved (see for example 11. Korytov, M., et al. *Use of the Belleville spring package in the vibration protection mechanism of the operator's seat*. in *Journal of Physics: Conference Series*. 2022. IOP Publishing.). Such approaches are not pursued in the present project but offer possibilities to consider in the future.

Belleville washers (referred to therein as coned disc springs) for vertically isolation of the reactor vessel and other components in a horizontally isolated nuclear power plant building was discussed in references [14-16]. Belleville washers have been used to maintain bolt tension in frictional sliding structural connections [17]. Shape memory Belleville washers have also been considered for energy-dissipating braces in structures [18]. The closely related concept of ring springs has been studied for seismic isolation in [19]. Use of Belleville washers for vertical isolation of buildings under train-induced vibration has been studied in [20]; in this paper, the different force-displacement responses of Figure 1-2 are properly utilized and a thorough analysis of hysteretic behavior (cf. Chapter 3 in this report) is presented.

The first suggestion of using Belleville washers for seismic protection of substation equipment was in a report prepared for Bonneville Power Administration [1]. The suggestion was made in the context of lightning arresters. The 1984 edition of IEEE 693 [21] briefly mentions the possibility of Belleville washers for seismic protection, but this was removed in subsequent edition. Seattle City Light has been installing Belleville washer stacks for seismic protection of their equipment; the present research was driven by this.

The goal of this project is to study the effectiveness of Belleville washers for seismic protection of equipment such as capacitive voltage transformers (CVT), capacitor banks etc. that do not have moving parts (such as in switches) and do not have complex dynamic modes of their own (such as dead tank circuit breakers). Such equipment, when mounted on support structures, essentially behave as rigid bodies rocking under horizontal ground motion due to the flexibility of the support structure. When Belleville washer stacks are installed at the base of such equipment, above the support structure, the equipment will rock under horizontal ground motion relative to the support structure. The Belleville washer stacks are expected to provide damping through frictional dissipation under such motion, resulting in reduction of equipment base moment relative when they are rigidly connected to the support structure. In deforming to provide frictional dissipation, the washer stacks will also invariably reduce the frequency; this reduction may further aid in reducing base moment. This could potentially occur at the expense of increased terminal deflection that must be accommodated.

The objectives of this project are:

1. Develop an analysis-based systematic approach for design of a Belleville-washer seismic protective system for a given equipment (together with given seismic demand and support structure).
2. Develop support for such an approach through physical experiments.

A CVT provided by Seattle City Light (see) is used in the shake table experiments described in Chapter 4.

Nomenclature for washer configurations

The specific washers used in the project are from Key Bellevilles [22] and are listed in Table 1-1.

Table 1-1
Washers used in this project [22]

Washer	Outer Diameter (in)	Inner Diameter (in)	t (in)	h (in)	Flattening load (lb)
K1875-G-086	1.875	0.656	0.086	0.043	1319
K1750-J-057	1.750	0.88	0.057	0.057	650

Table 1-2 summarizes the nomenclature used in this report for Belleville washer units, each consisting of series parallel arrangements. A stack is identified by the number and type of units, for example as illustrated in Table 1-2.

Table 1-2
Nomenclature used for Belleville washer units and stacks

Units		Stack
	Configuration	Nomenclature
1		1U
2		1D
3		1U1D
4		2U2D
5		3U3D

Example: Stack consisting of 2 units of 2U2D

Then washers are nested with the cones oriented in the same direction, as for example in the top or bottom half of a 2U2D unit, they act in *parallel* since when a load is applied, their deformations are the same. When the cone orientations are opposite, as for example with the two washers in a 1U1D unit, they are in *series*, since they see the same force and their deformations are additive. Thus, a stack can be viewed as a series-parallel arrangement of washers. If the washers were ideal springs, the stiffness of a stack can be calculated using series-parallel combinations of the stiffnesses of the constituent springs (as will be seen in Chapter 3, washers,

particularly when nested are not linear springs and exhibit hysteresis, so such a calculation of stiffness would only be approximate). The strength (flattening load) of a stack is determined by the weakest parallel combination in the stack.

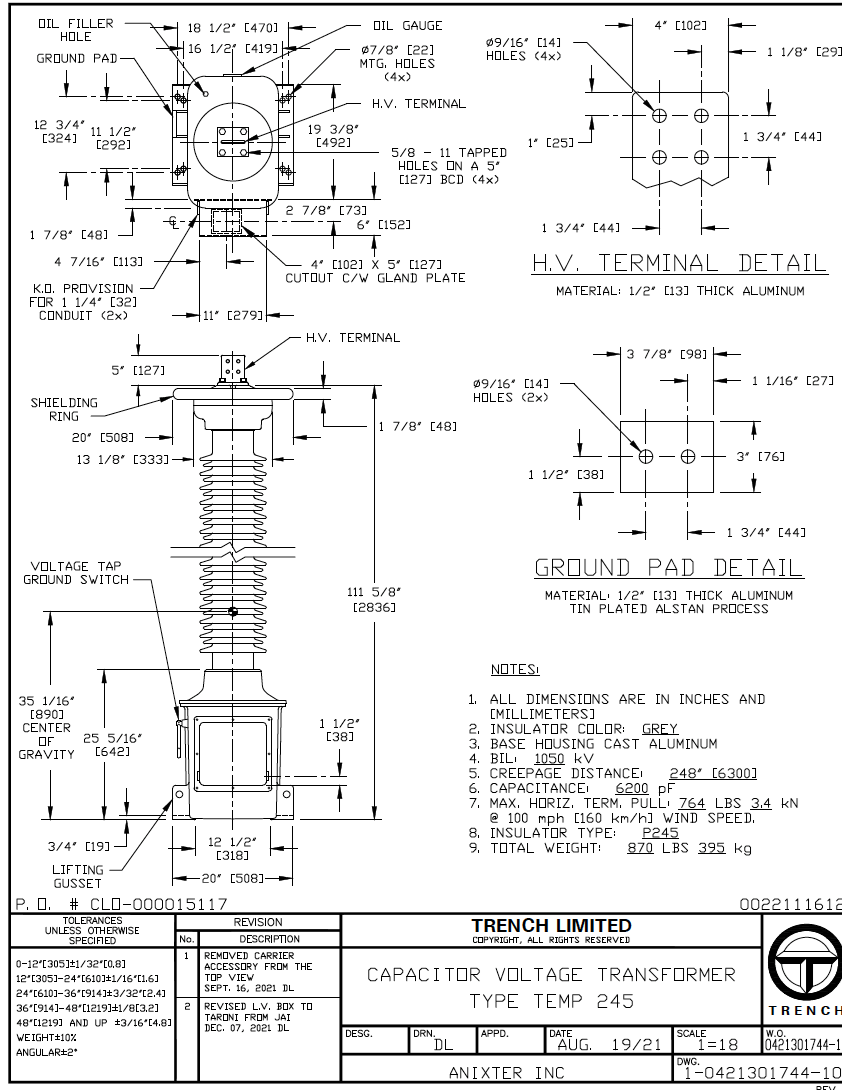


Figure 1-3
Capacitive voltage transformer (CVT) provided by Seattle City Light and used in shake table experiments described in Chapter 4.

Analysis and design questions

The findings reported here must ultimately guide the selection of washer stacks the provide the desired level of seismic protection. This is the design question, given (a) an equipment, (b) its support structure, (c) seismic input (design spectrum) and (d) performance specifications (max base moment, max terminal displacement etc.), design a Belleville washer stack so that the system response meets the specifications.

A prerequisite to approaching this design question is being able to answer the analysis question, given (a) an equipment, (b), its support structure, (c) seismic input (ground motion record) and

(d) a specific Belleville washer configuration, compute the response of this system (accelerations, base moments, terminal displacements etc.). Hence the emphasis of this project is more on this analysis question and support for the analysis process from physical experimental measurements, with a focus as noted above on “rigid” structures, in particular a CVT.

Organization of the report

This report is organized as follows. As noted above, the main goal of this project is to develop an analysis-based systematic approach for design of a Belleville-washer seismic protective system. The report is therefore structured around an analysis procedure. This procedure is summarized upfront in Chapter 2, and the various steps in this procedure are expounded in subsequent chapters. Characterizing the force-displacement hysteresis of a single stack of washers through cyclic loading tests is presented in Chapter 3. Shake table experiments to characterize dynamic seismic response of a CVT equipment with Belleville washer stacks, including setup, instrumentation and specific steps for installing the washer stacks, are described in Chapter 4. In Chapter 5, a nonlinear dynamic model of the CVT with Belleville washer stacks is developed, and predictions from the model are compared with measurements from shake table experiments. An important note is that all the information needed for this model can be obtained from the washer characterization data from Chapter 3, the type of information that can be readily obtained. In Chapter 6, a linearized model based on equivalent stiffness and damping is developed that may be more conducive for practical use than the nonlinear model in Chapter 5; this linear model can also be developed simply for the characterization data in Chapter 3. The approach taken in this report to analyze substation equipment with Belleville washer seismic protective systems loosely parallels that in ASCE 7 for seismically isolated structures; this is pointed out in Chapter 6 to lend credence to the proposed approach relative to well-established procedures in seismic standards. Finally in Chapter 7, a summary is provided, and some outstanding questions are identified.

2

PROPOSED ANALYSIS PROCEDURE

The main goal of this project is to develop an analysis-based systematic approach for design of a Belleville-washer seismic protective system. Therefore, in this chapter, a proposed analysis procedure is laid out. This serves to tie together the different steps and experimental support for these steps discussed in subsequent chapters. The following is the proposed analysis procedure:

Given (a) an equipment, (b) its support structure, (c) seismic input (ground motion record), (d) Belleville washer configuration

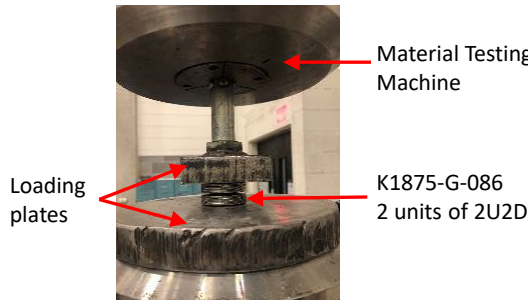
1. Determine the force-displacement response of the stack.
 - In this project, we have done this by testing the stack in a material test machine (see Chapter 3).
 - This is a hysteretic behavior.
2. Compute the moment-rotation behavior of the assembly of washer stacks (see Chapter 5).
 - This can be done, for example, in an Excel spreadsheet.
 - In this project, special instrumentation has been used to experimentally verify the relationship between the stack force-displacement behavior and the system moment-rotation behavior (see Chapter 4).
3. Model this moment-rotation behavior – two possible approaches.
 - Fit a hysteresis model (Chapter 5).
 - Compute an “equivalent” stiffness and damping (Chapter 6).
 - Both approaches have been verified in this project; it has also been verified that this equivalent stiffness and damping agrees well with fitting a linear model to the measured response.
4. Compute the system response – three approaches are possible.
 - Nonlinear time-history analysis with the hysteresis model for the washer arrangement (Chapter 5).
 - Linear time history analysis with the equivalent stiffness and damping.
 - Response spectrum analysis with the equivalent stiffness and damping ((Chapter 6). This together with the equivalent stiffness and damping resemble ASCE 7 process for base isolation (Chapter **Error! Reference source not found.**)).
 - In the project, it has been verified that the three approaches produce close responses

3

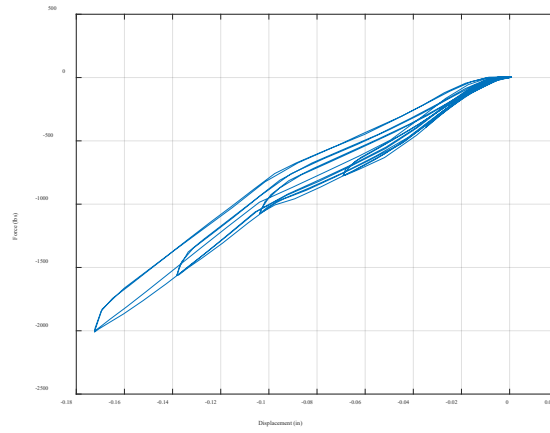
CYCLIC FORCE-DISPLACEMENT BEHAVIOR OF WASHER STACKS

This chapter is on the measurement of force-displacement behavior of Belleville washer stacks. As will be seen in Chapters 5 and 6, this is the primary information required to predict the seismic response of rigid equipment (besides mass, moment of inertia of the equipment itself and support structure stiffness).

The force displacement response of a washer stack is obtained here by applying cyclic compressive loading to the stack in a materials testing machine. At first, this was done by simply compressing the stack between loading plates as shown in Figure 3-1(a). The resulting force-displacement curves of Figure 3-1(b) showed changes in slope that weren't observed in force-displacement measurements of the same stack in shake table tests (the special instrument designed to measure this response *in situ* under the equipment in the shake table test is discussed in Chapter 4). This is likely because of slight misalignment between washers in the stack initially that corrects itself during the loading. To avoid this, an alternative approach was devised, where the compressive loading was applied to the stack through a loading frame and guiding rod as illustrated in Figure 3-2(a). This arrangement is closer to how the washer stack is installed under the equipment. The guiding rod prevents any initial misalignment and subsequent realignment. The resulting force-displacement measurement, shown in Figure 3-2(b), does not have any unexpected changes in slope. Indeed the *in situ* measurements from the shake table tests follow these curves closely as seen in Figure 3-3.

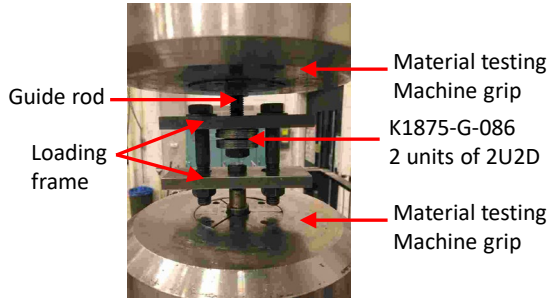


(a) Washer stack compressed directly between loading plates

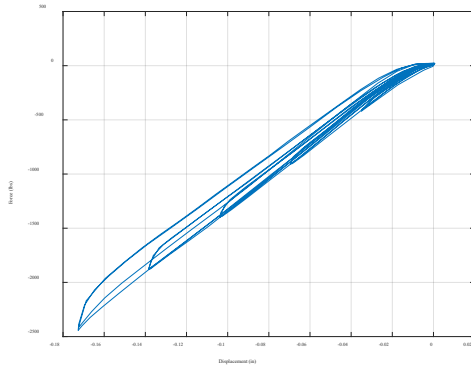


(b) Measured force-displacement hysteresis

Figure 3-1
Washer stack force-displacement response measurement by *compressing the stack directly* in the materials testing machine; force-displacement response exhibits unexpected changes in slope.



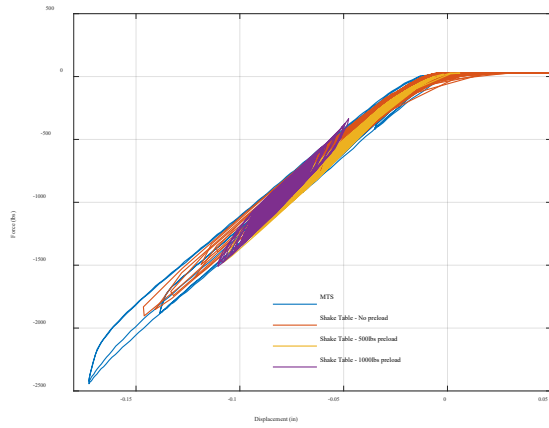
(a) Washer stack compressed through a loading frame with guiding rod



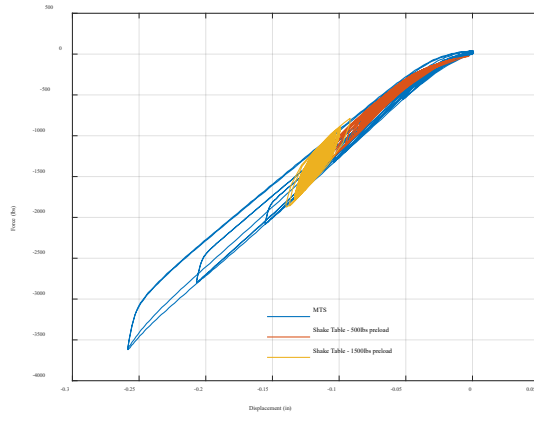
(b) Measured force-displacement hysteresis

Figure 3-2

Washer stack force-displacement response measurement by *compressing the stack through a loading frame with guiding rod*; this is closer to how washers are mounted under the equipment, and the force-displacement response is clean.



(a) 2 units of 2U2D K1875-G-086

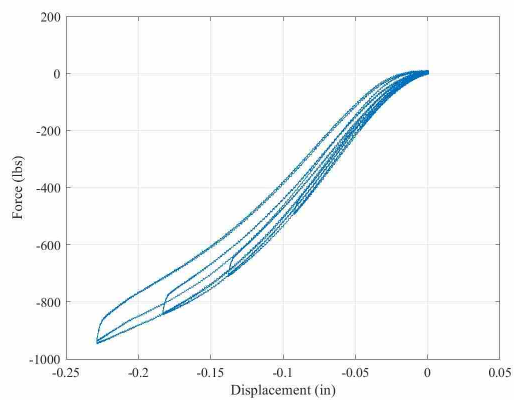


(b) 3 units of 3U3D K1875-G-086

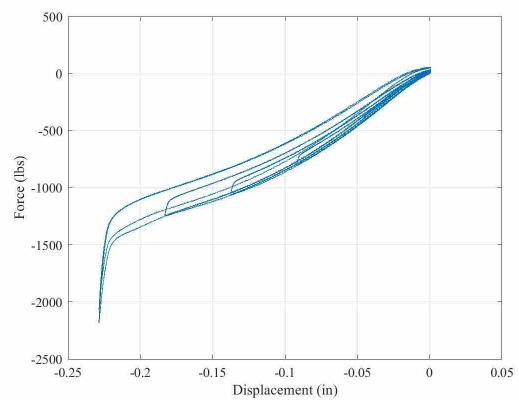
Figure 3-3

Measured force-displacement curves for two configurations. The legend MTS denotes measurement from the materials testing machine through the frame with guiding rod. The other curves are in situ measurements from the shake table at different preload levels. The in situ measurements follow the testing machine results closely, confirming that the washer stack response can be characterized fully using simply a materials testing machine.

Figure 3-4 shows force-displacement curves for two configurations of the K1750-J-057 washers. They exhibit the reduction in stiffness with loading noted in Figure 1-2 due to their higher h/t ratio.



(a) 2 units of 2U2D K1750-J-057



(b) 2 units of 3U3D K1750-J-057

Figure 3-4

Measured force-displacement curves for two configurations with the K1750-J-057 washers. They have a softening behavior because of their larger h/t ratio (cf. Figure 1-2)

4

SHAKE TABLE EXPERIMENTS

In this chapter, shake table experiments on the CVT equipped with Belleville washer stacks are described. The experimental setup, instrumentation, and washer installation process are detailed. The primary purpose of these experiments is to obtain measurements in support of the analysis procedure outlined in Chapter 2. Consequently, special instruments were used to measure the washer response in situ. Instrumentation was also designed with redundancy in mind, so that the same quantity is measured by multiple means and can be cross-checked. Some other checks such as sums of forces or moments are performed to confirm the integrity of the measurements.

Test setup

Figure 4-1 shows the CVT mounted on the shake table. The CVT is mounted on a pedestal referred to as the “spool”, which in turn is mounted on the shake table. The spool consists of a 10-in diameter $\frac{1}{2}$ -in thick 16.5-in tall steel tube with a 22in \times 17 steel plate welded on top (to match the base dimensions of the CVT). Figure 4-1 also shows the direction convention X along the East-West direction, Y along the North-South direction and Z along the vertical direction. The distance between the mounting holes at the base of the CVT is greater in the Y direction than in X direction (resulting, for example, in the Y frequency direction than in the X direction). The Belleville washer stacks are installed between the CVT base and the spool, details of which are elaborated below.

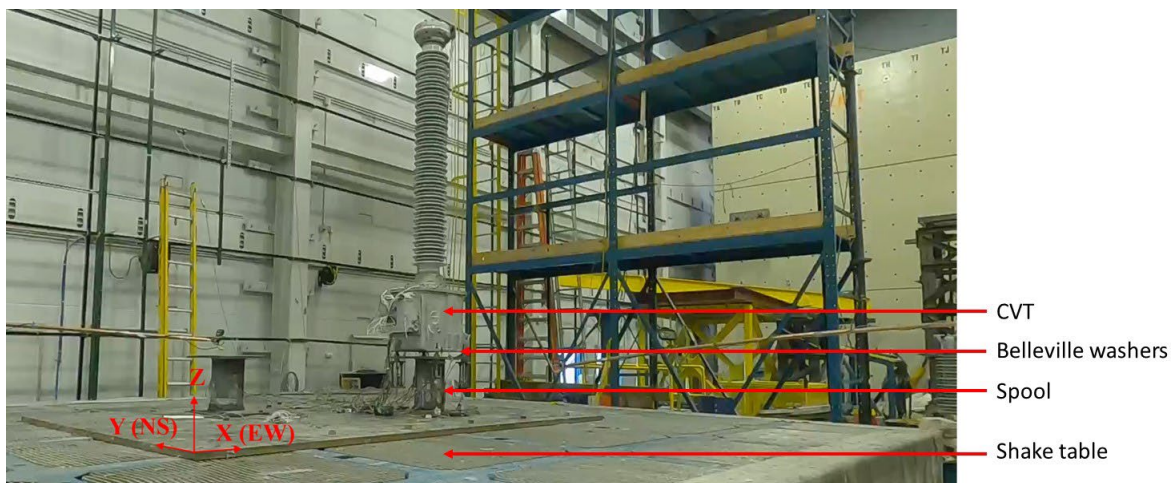
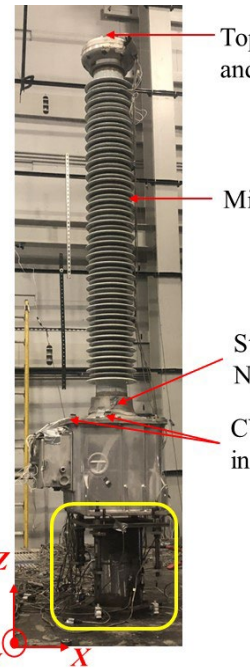


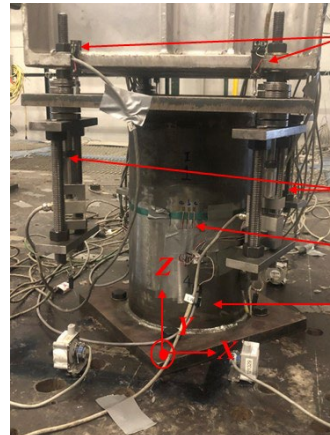
Figure 4-1
CVT mounted on shake table

Instrumentation

An overview of response quantities measured and corresponding instrumentation is provided in Figure 4-2. Table 4-1 contains a detailed summary. In addition to these response quantities that are measured directly, further response quantities are derived indirectly from them. These quantities as well as the process used to derive them are summarized in Table 4-2. A specialized instrument in Table 4-1, designed in this project to measure the force in a washer stack in situ is



(a) Summary of instruments



(b) Closeup of yellow box in (a)

Figure 4-2
Instrumentation details

Table 4-1
Summary of measured response quantities and corresponding instruments

	Response quantity	Instrument
1	Top X and Y displacement components	String potentiometers attached to frames outside the shake table, so these measure absolute displacements
2	Top X and Y acceleration components	One 3D accelerometer
3	X and Y accelerations at insulator mid-height	Two 1D accelerometers
4	Z accelerations at N,S,E,W locations on CVT box	Four 1D accelerometers
5	Insulator base moment	Strain gages at N,S,E,W locations at insulator base, calibrated to measure base moment
6	Displacements at 4 locations of the base of the CVT relative to the spool plate	Four linear potentiometers
7	Tension forces in rods going through the four washer stacks	Four specially designed instruments called “load washer alternates” LWAs (see below)
8	Two bending moment components in the spool (M_{spool})	Two full-bridge strain gage circuits, one for X bending moment and the other for Y
9	Shake table accelerations	Accelerometers
10	Shake table displacements	String potentiometers

Table 4-2
Response quantities derived indirectly from measurements

	Derived response quantity	Symbol*	Method of computation
i	Rigid-body translational and rotational acceleration of CVT at center of mass	$\ddot{x}_t, \ddot{\theta}$	Linear fit to acceleration components rows 2–4 in Table 4-1. A good fit here demonstrates the CVT can be idealized as a rigid body.
ii	Total rotation of CVT	θ	Linear fit to CVT displacements (row 1) and shake table displacements (row 10) in Table 4-1
iii	Rotation of CVT relative to spool plate	θ_w	Linear fit to displacements in row 6 of Table 4-1
iv	Restoring moment generated by washer stacks (and spool plate)	M_{CVT}	Twice the moment computed from the four LWAs (row 7 of Table 4-1, see Figure 4-3 for details)
v	Deflection of spool plate	-	Difference of rows ii and iii above

* the symbols listed here are in reference to dynamics in the X East-West direction, corresponding quantities in the Y North-South direction will be labeled similarly, but not shown here

the Load Washer Alternate (LWA) shown in Figure 4-3. It consists of a frame made of a frame consisting of two plates and two $\frac{3}{4}$ -in threaded rods. The guiding rod of the Belleville washer stacks goes through a hole in the top plate, and connects to a load cell attached to the bottom plate. When the washer stack right above the top plate is compressed, the guiding rod develops tension that is measured by the load cell. Thus the load cell measures the compression in the Belleville washer stack below the spool plate.

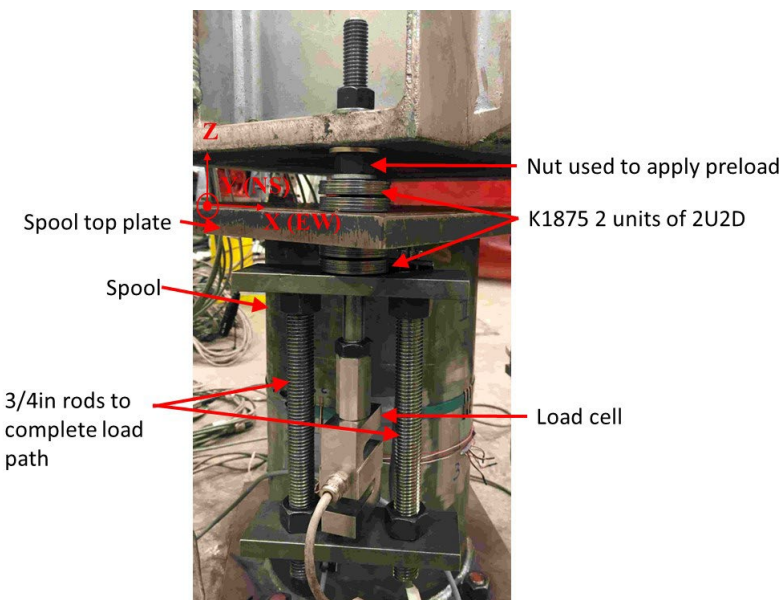


Figure 4-3
Details of Load Washer Alternate (LWA) and preloading process

Determination of CVT inertia properties

For further analysis, the mass, mass moment of inertia and center of mass position of the CVT must be determined. The mass is obtained simply from the measured weight. The center of mass position is determined by balancing the CVT horizontally using a crane. The mass moment of inertia is computed from the frequency measured by mounting the CVT on springs of known stiffness (Figure 4-4) using the method outlined in Figure 4-5. A summary of the inertia properties of the CVT is shown in .

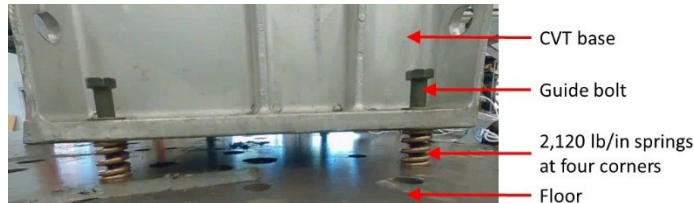


Figure 4-4
CVT mounted on springs to estimate mass moment of inertia indirectly from measured frequency

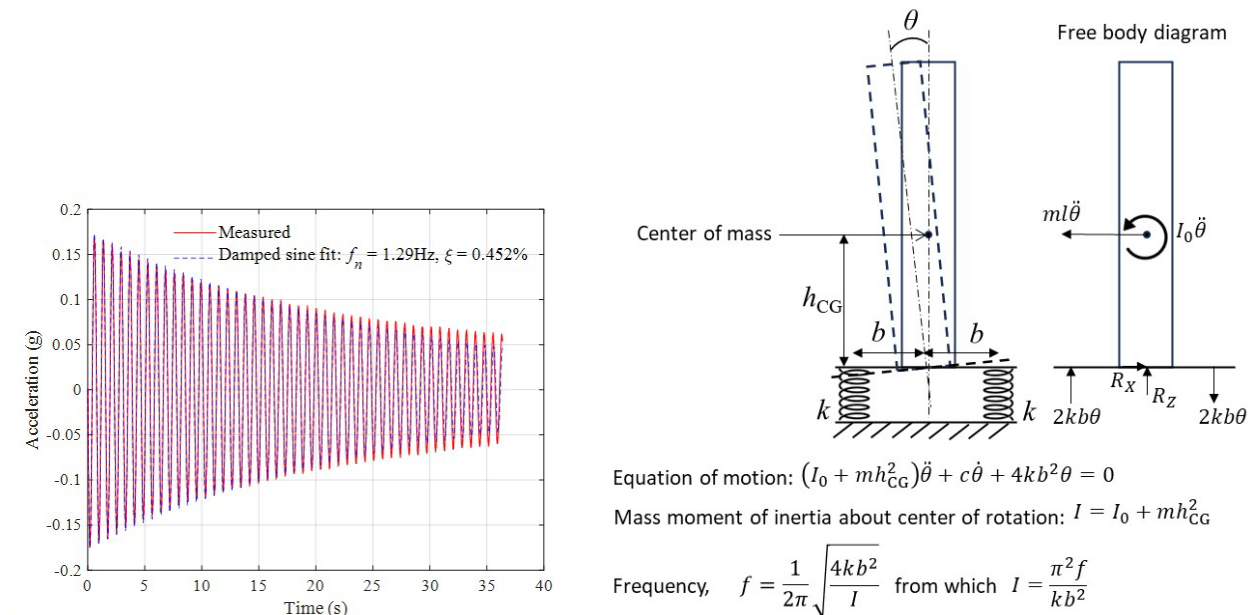


Figure 4-5
Acceleration measured when CVT is mounted on springs and the resulting frequency fit, and process to compute CVT mass moment of inertia from measured frequency; the dimension b is 6.375in in the X direction and 9.25in in the Y direction.

Table 4-3
Summary of CVT inertia properties

Parameter	Description	Value
m	Mass	940/386.4 lb-s ² /in
h_{CG}	Height of center of mass from CVT base	35-1/16 in
I	Mass moment of inertia about center of rotation	5,500 lb-s ² -in
I_0	Mass moment of inertia about center of mass	2,500 lb-s ² -in

Washer stack installation

Special care is exercised in controlling the preload when installing the Belleville washer stacks. The stacks are installed on the spool plate with out the CVT present. The stacks at each corner are preloaded independently by tightening the nut at the top (Figure 4-3) by a prescribed number of turns corresponding to fraction of flattening displacement targeted in the washer stacks. The force in the bottom stack is simultaneously monitored using the LWA to make sure that the load corresponds to the stack deflections in accordance with the force-deformation relationship measured in the tests described in Chapter 3. The CVT is then seated on the four top nuts, and fixed in place using four nuts above the CVT base plate.

Test configurations and protocol

Pull tests were performed in the *X* and *Y* directions with the CVT fixed directly to the spool plate to calibrate to the bending moment load cells in the spool and the strain gages at the insulator base to bending moment.

The washer configurations shown in Table 4-4 were tested. All configurations were double acting – there were washer stacks above and below the spool plate.

Table 4-4
Summary of configurations tested

Washer type	Configuration	Pre-load (% of flattening)
K1875-G-086	2 units of 2U2D	0 lb (0%)
		500 lb (25%)
		1,000 lb (50%)
	3 units of 3U3D	500 lb (17%)
		1,500 lb (50%)

For each configuration, a sequence of tests consisting of low-level broad-band random input (for baseline system identification) and the CERL ground motion with increasing amplitude levels (culminating at 0.5g) were applied first in the *X* direction and then in the *Y* direction. The 5%-damped test response spectra of the applied motion are shown in .

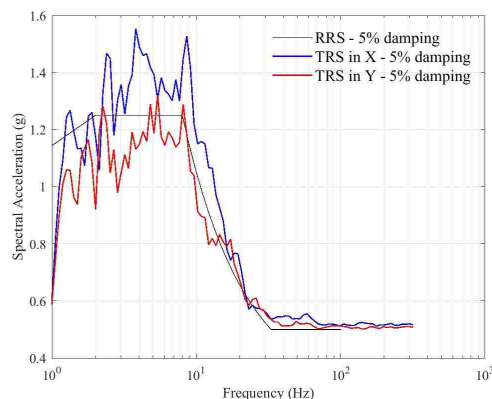


Figure 4-6
5%-damped test response spectra of applied CERL motion compared with required response spectrum

Correlating measured forces and accelerations

Various measured forces and accelerations are correlated to gain confidence in the measurements to then compare with analysis predictions in Chapter 5.

Consider the free body diagram in Figure 4-7. The dimensions used in this free body diagram are summarized in Table 4-5. The equilibrium equations are

$$\begin{aligned}\sum F_x = 0 &\Rightarrow V = m\ddot{x}_t \\ \sum M = 0 &\Rightarrow M_{\text{spool}} = -I_0\ddot{\theta} - VL = -I_0\ddot{\theta} - m\ddot{x}_t L\end{aligned}\quad (4-1)$$

The correlation between the left and right hand sides of the second of equations (4-1), each of which is obtained using independent measurements, is verified in Figure 4-8, demonstrating consistency.

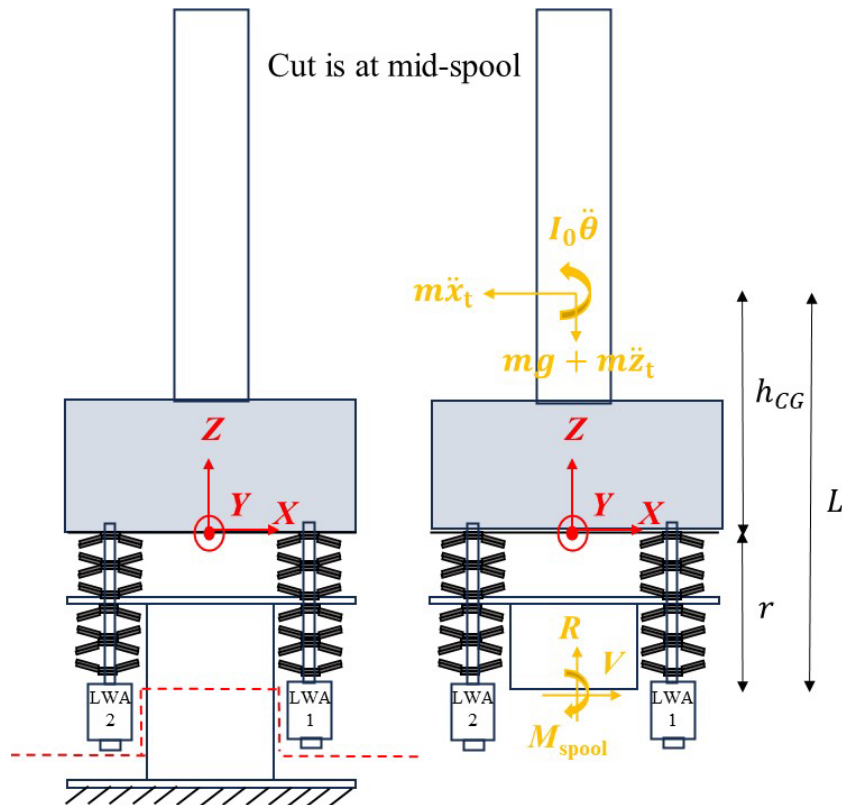


Figure 4-7
Free body diagram with mid-spool cut

Table 4-5
Summary of CVT inertia properties

Dimension	Description	Value
r	Distance between CVT base and mid spool	11 in
L	Distance between CVT center of mass and mid spool	46-1/16 in
l	Distance between CVT center of mass and center of rotation; this is obtained by fitting the equation $\ddot{x}_g + \ddot{\theta} = \ddot{x}_t$	38 in

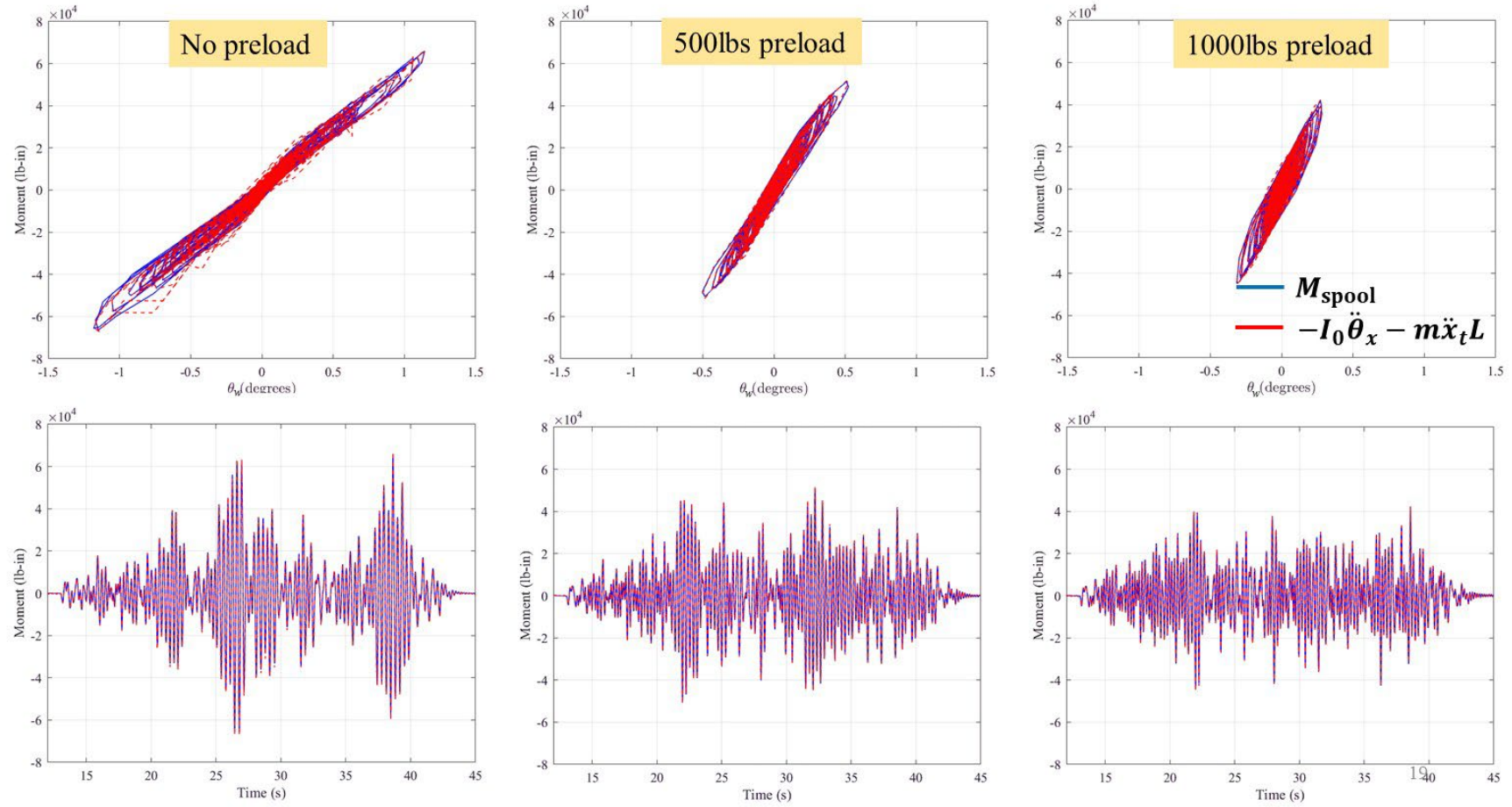


Figure 4-8
Correlation between the independent measurements, M_{spool} and $-I_0 \dot{\theta} - m \ddot{x}_t L$, demonstrating consistency for the 2 units of 2U2D configuration under 0.5g CERL motion in the X direction.

Next consider the free body diagrams shown in Figure 4-9. In this figure, F_{it} and F_{ib} stand for the force in the top and bottom washer stacks at corner i , and F_i for the force in the corresponding guide rod. Superscript “pre” denotes the preload component of these forces and Δ denotes the change due to the CVT weight and during dynamic response. Since each assembly of washers under preload is in equilibrium,

$$F_{ib}^{\text{pre}} = F_{it}^{\text{pre}} = F_i^{\text{pre}} \quad (4-2)$$

Furthermore,

$$F_1^{\text{pre}} = F_2^{\text{pre}} = F_3^{\text{pre}} = F_4^{\text{pre}} \quad (4-3)$$

since all the assemblies are preloaded to the same level. Summing moments about the center of rotation O ,

$$\begin{aligned} M_{\text{spool}} - (F_1^{\text{pre}} + \Delta F_1 + F_4^{\text{pre}} + \Delta F_4)b + (F_2^{\text{pre}} + \Delta F_2 + F_3^{\text{pre}} + \Delta F_3)b \\ + (F_{1t}^{\text{pre}} - \Delta F_{1t} - F_{4t}^{\text{pre}} - \Delta F_{4t})b - (F_{2t}^{\text{pre}} - \Delta F_{2t} - F_{3t}^{\text{pre}} - \Delta F_{3t})b - Vr = 0 \end{aligned}$$

Using (4-2) to cancel out the F_i^{pre} and F_{it}^{pre} terms, and substituting for V from (4-1),

$$M_{\text{spool}} - (\Delta F_1 + \Delta F_4)b + (\Delta F_2 + \Delta F_3)b - (\Delta F_{1t} + \Delta F_{4t})b - (\Delta F_{2t} + \Delta F_{3t})b - m\ddot{x}_t r = 0 \quad (4-4)$$

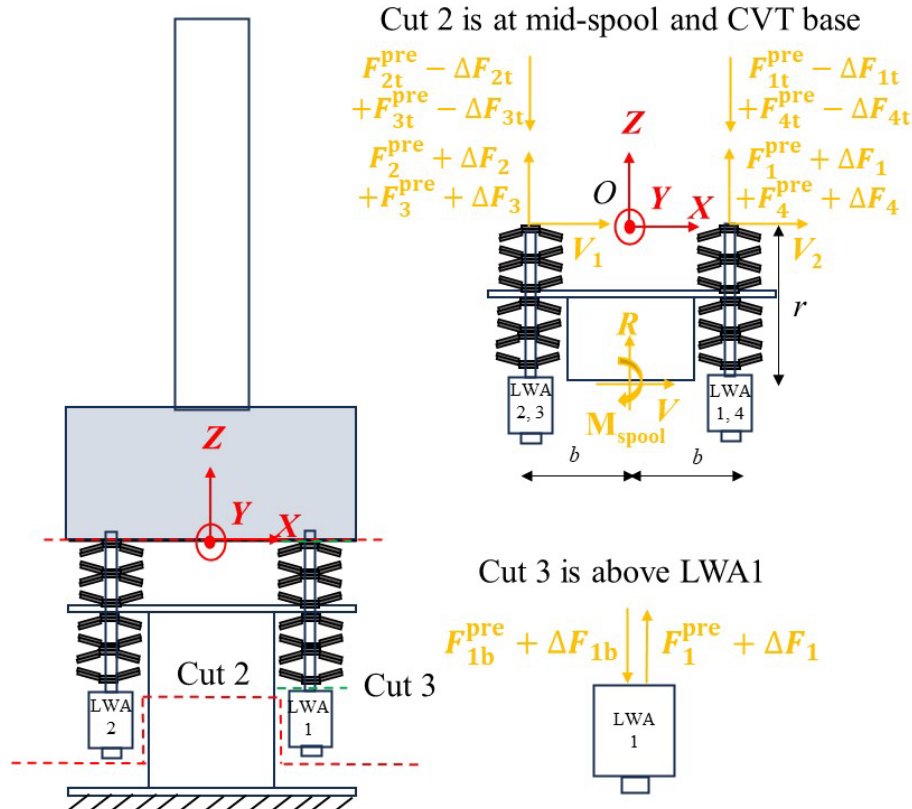


Figure 4-9
Free body diagrams relating moment measured at the spool with moment estimated using LWAs

A further assumption is made that

$$\Delta F_i = \Delta F_{ib} = \Delta F_{it} \quad (4-5)$$

This does not follow from equilibrium, but is taken to be true based on symmetry/compatibility of top and bottom stack deformations. Then equation (4-4) becomes

$$M_{\text{spool}} = 2(\Delta F_1 + \Delta F_4 - \Delta F_2 - \Delta F_3)b + m\ddot{x}_t r \quad (4-6)$$

Using equation (4-3), this can be further written as

$$M_{\text{spool}} = \underbrace{2(F_1 - F_2 - F_3 + F_4)b}_{M_{\text{CVT}}} + m\ddot{x}_t r \quad (4-6)$$

where $F_i = F_i^{\text{pre}} + \Delta F_i$ is the directly the force measured by LWA i . Verifying this relationship, which again involves multiple independent measurements, adds further confidence in the measured data for comparison with analysis. In particular, this confirms the thinking that the in situ behavior of the washer stacks can be determined from the materials testing machine measurements. This comparison is shown in Figure 4-10.

A final free body diagram, Figure 4-10, is considered in relation to the insulator base moment. The mass and mass moment of inertia of the insulator alone are not known, however its center of mass is assumed to be at mid-height. Summing the moments about the insulator base,

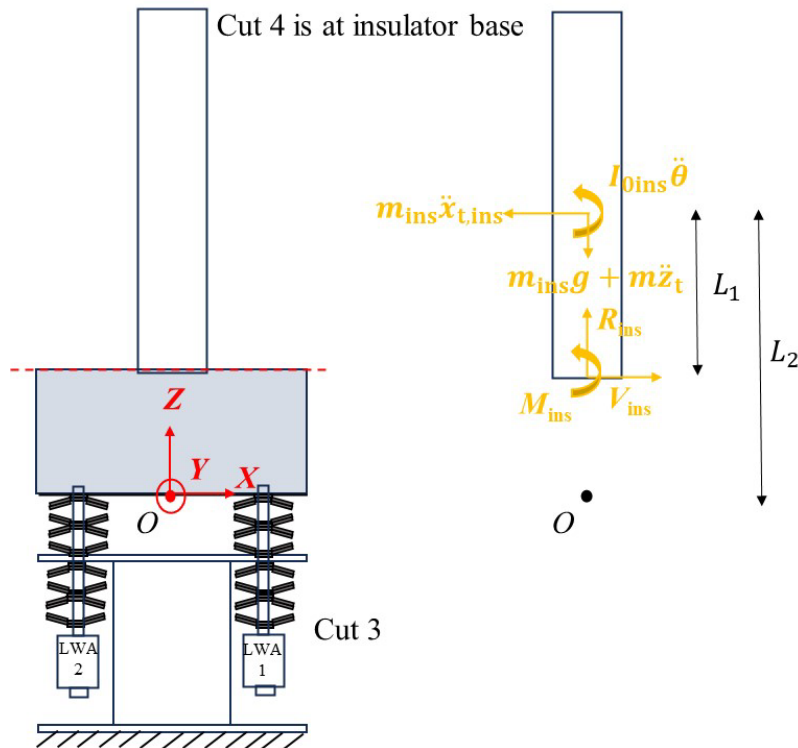


Figure 4-10
Free body diagram used to relate insulator base moment to measured accelerations; L_1 is the mid-height of the insulator, $L_1 = \text{in}$; L_2 = the distance from the center of rotation to the center of mass

of the insulator, $L_2 = \text{in.}$

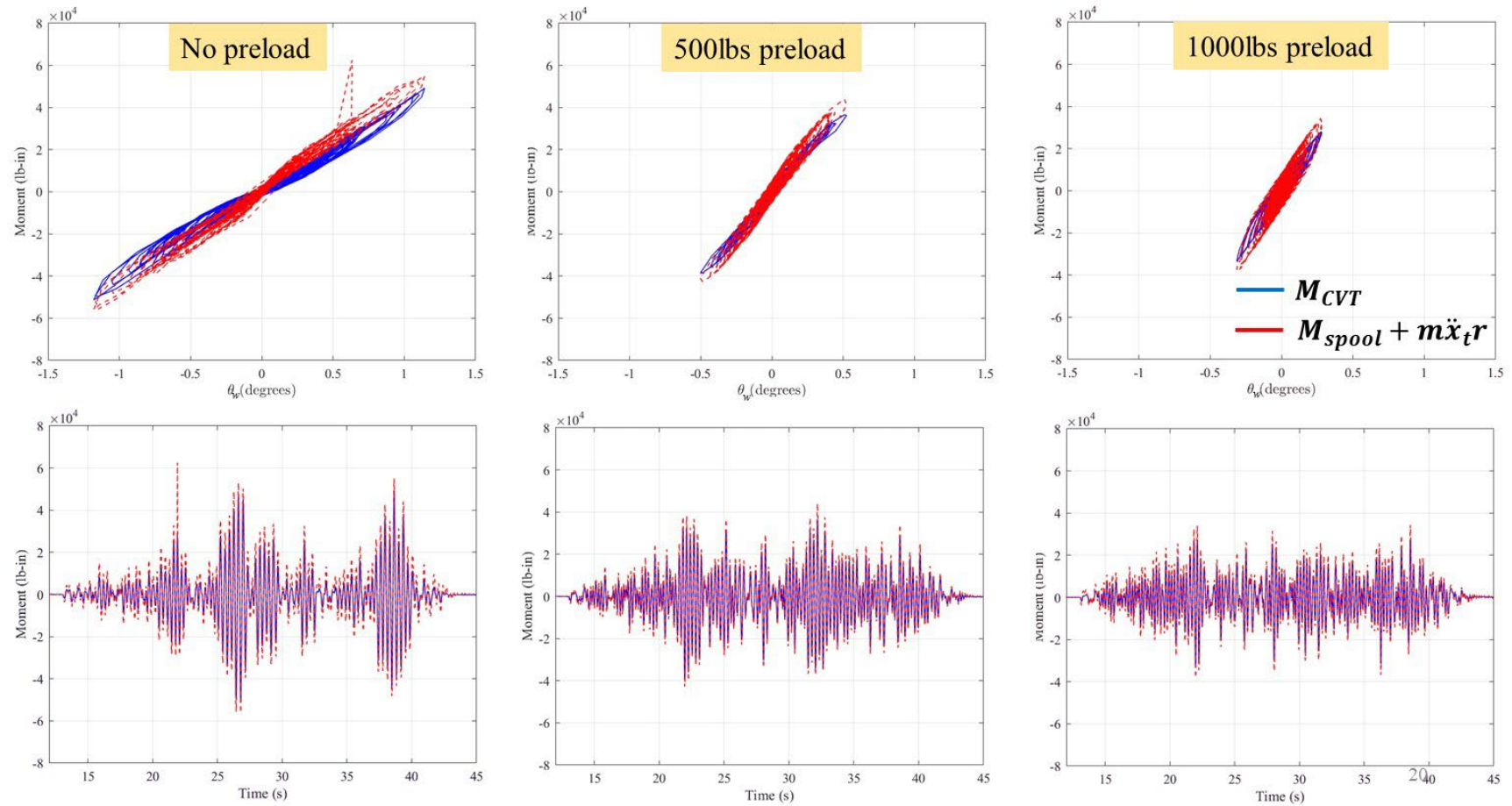


Figure 4-11
Correlation between M_{spool} and M_{CVT} per equation (4-6) demonstrating consistency for the 2 units of 2U2D configuration under 0.5g CERL motion in the X direction.

$$M_{\text{ins}} = -I_{0\text{ins}} \ddot{\theta} - m_{\text{ins}} \ddot{x}_{t,\text{ins}} L_1 \quad (4-7)$$

Substituting the kinematics, $\ddot{x}_{t,\text{ins}} = \ddot{x}_g + L_2 \ddot{\theta}$,

$$M_{\text{ins}} = -\underbrace{(I_{0\text{ins}} + m_{\text{ins}} L_1 L_2)}_{I_{\text{ins}}} \ddot{\theta} - m_{\text{ins}} L_1 \ddot{x}_g \quad (4-8)$$

The insulator mass, m_{ins} , and the net mass moment of inertia, I_{ins} are known. Equation (4-8) is used to fit them to measure data. The fit values are $m_{\text{ins}}=360/386.4 \text{ lb-s}^2/\text{in}$ (about 40% of the total mass of the CVT) and $I_{\text{ins}}=3,500 \text{lb-in-s}^2$. These values are used when comparing analysis results to measured insulator base moment. The measured insulator base moments are shown in Figure 4-12 and Figure 4-13.

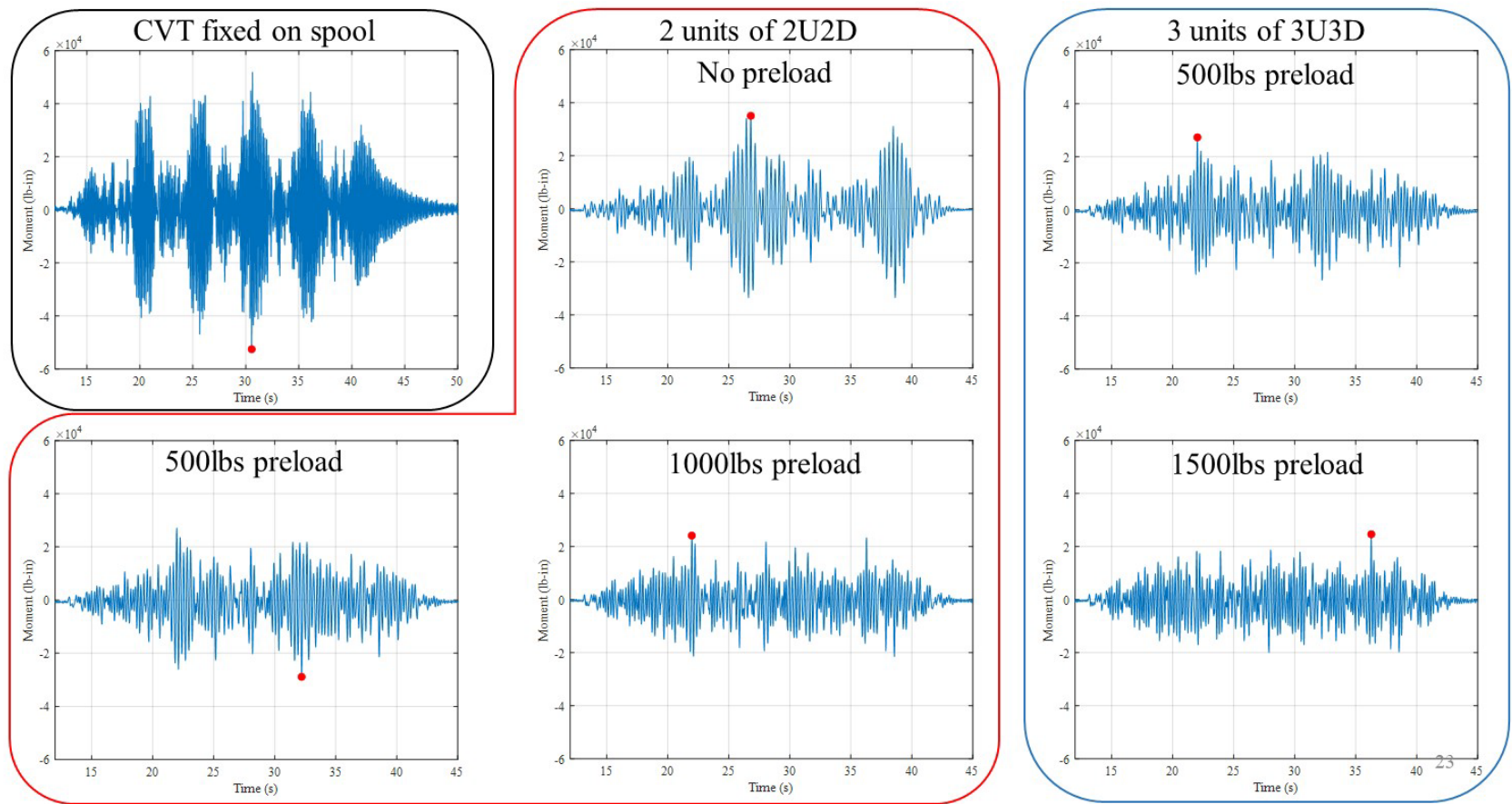


Figure 4-12
Measured insulator base moment for the different configurations for 0.5g CERL motion applied in the X direction

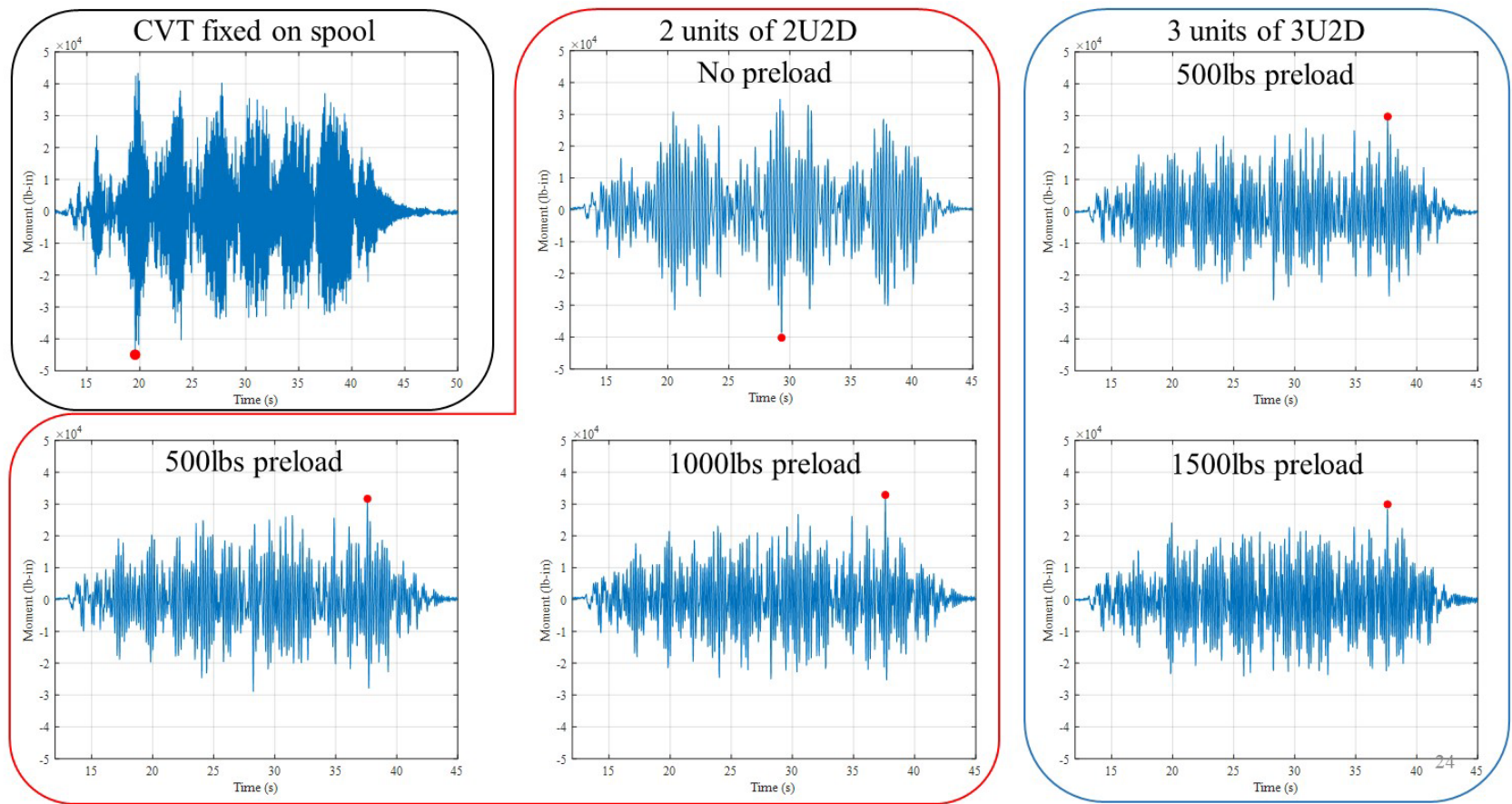


Figure 4-13
Measured insulator base moment for the different configurations for 0.5g CERL motion applied in the Y direction

5

NONLINEAR MODELING AND ANALYSIS

In this chapter, a nonlinear model is developed for the CVT installed on Belleville washer stacks. The CVT is modeled as a rigid body, and a hysteretic model is used to represent the moment-rotation behavior resulting from the aggregate action of the washer stacks (the type of moment-rotation hysteretic behavior seen in the measurements of Figure 4-11).

From stack force-displacement to system moment-rotation

The moment-rotation hysteresis behavior can be obtained from the washer stack force-displacement response, whose measure was discussed in Chapter 3, using the process depicted in Figure 5-1. An example of this process is illustrated in Figure 5-2. The specific example shown in Figure 5-2 corresponds to a low preload (25% of flattening). In this condition, when the

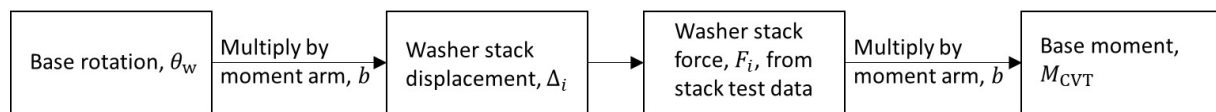


Figure 5-1
Process to obtain moment-rotation behavior from washer-stack force displacement behavior

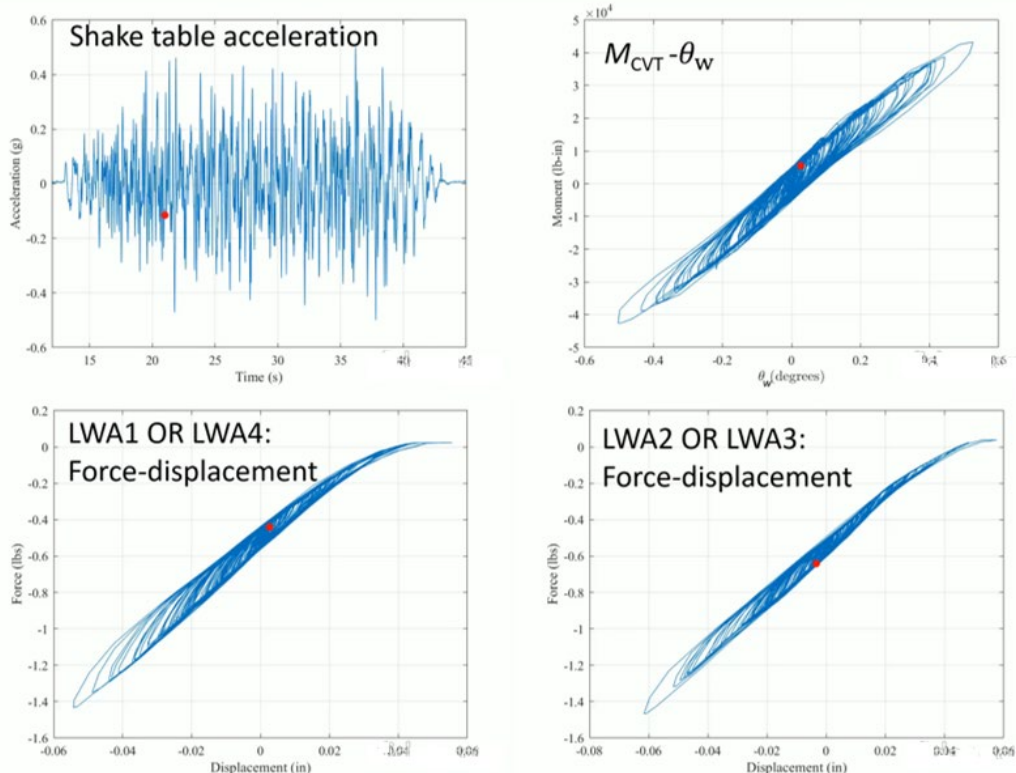


Figure 5-2
Example of constructing the moment-rotation behavior from the stack force-displacement behavior for 2 units of 2U2D.

washer stacks on one side reach the highest deformation (bottom left of Figure 5-2), the stacks on the other side relax entirely, losing preload (bottom right of Figure 5-2). The net effect is a softening of the moment-rotation behavior near the extremes (top right of Figure 5-2).

Modeling moment-rotation hysteresis

The moment-rotation behavior decomposed into two parallel components – one elastic and one hysteretic as illustrated in Figure 5-3. The split is given by

$$M_{CVT} = K\theta_w + M_{HYS} \quad (5-1)$$

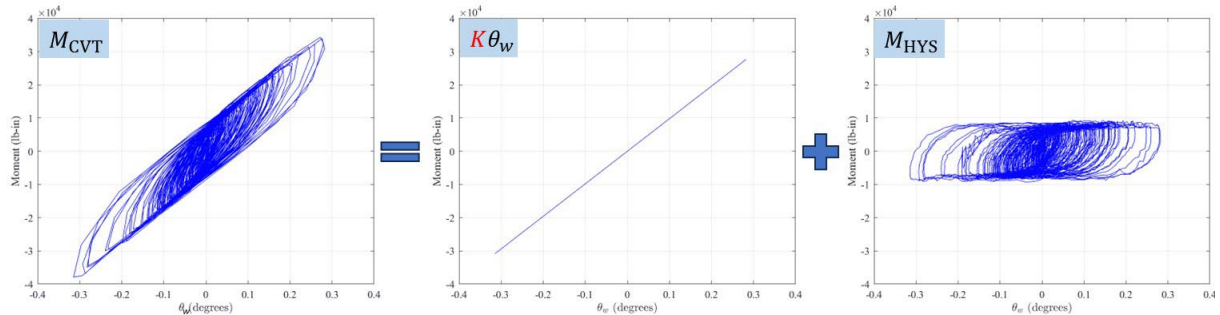
for cases with sufficient preload as in Figure 5-3(a) and by

$$M_{CVT} = K \tanh(\alpha\theta_w) + M_{HYS} \quad (5-2)$$

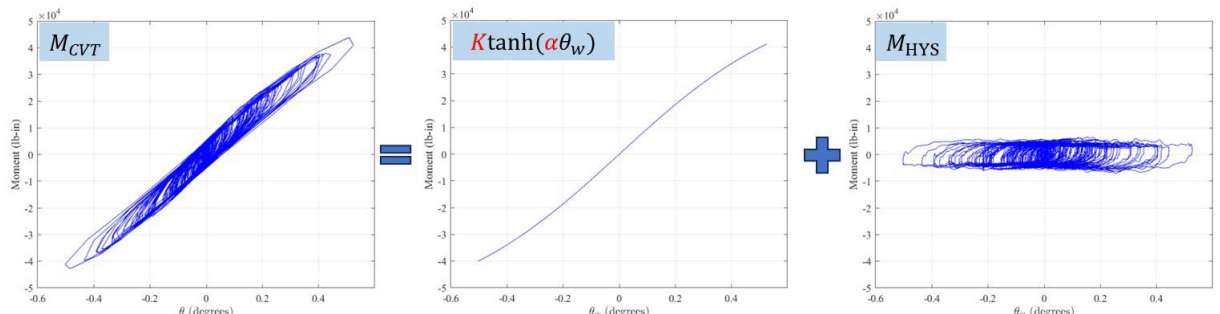
for cases with insufficient preload as in Figure 5-3(b), the tanh function capturing the S shape.

The hysteretic component is represented using what is commonly referred to as the Bouc-Wen model [23, 24] (for a description of this model using notation similar to that used here, see [25, 26]), and is given by

$$\dot{M}_{HYS} = k \left(1 - \left| \frac{M_{HYS}}{M_{yield}} \right|^N (\eta + (1 - \eta) \operatorname{sgn}(M_{HYS}\dot{\theta}_w)) \right) \dot{\theta}_w$$



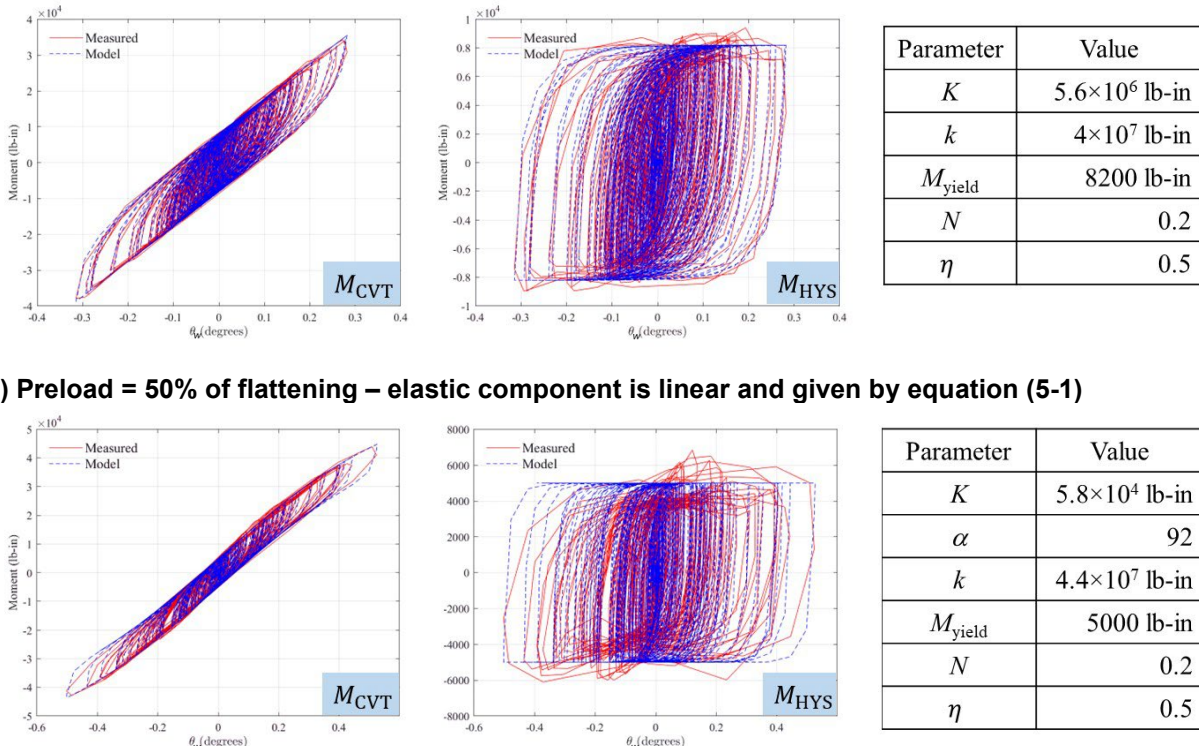
(a) Preload = 50% of flattening – elastic component is linear



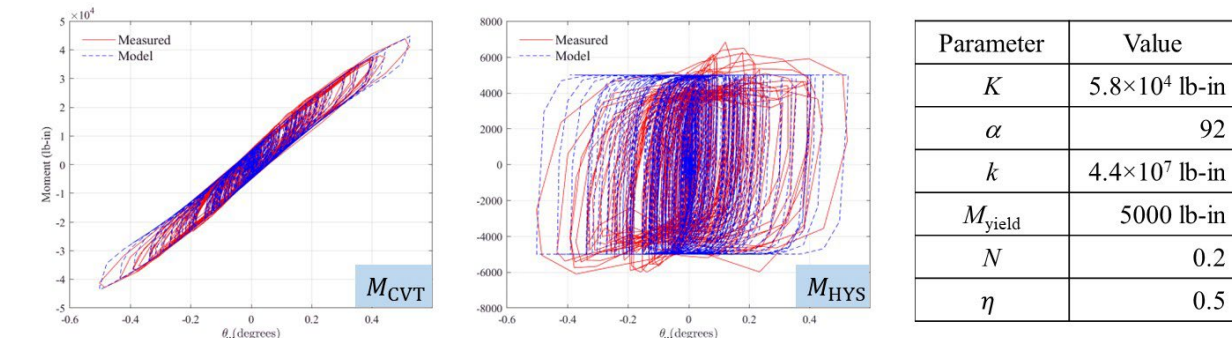
(b) Preload = 25% of flattening – elastic component is S-shaped due to the washer stacks on one side losing preload

Figure 5-3
Parallel decomposition of moment-rotation behavior into elastic and hysteretic components (example shown for 2 units of 2U2D).

where M_{yield} is the yield moment, and N and η are parameters that control the shape of the hysteresis. For an explanation of these parameters, see [27]. Figure 5-4 shows a comparison of the model with the measured moment-rotation behavior when the model is driven by the measured rotation of the CVT relative to the spool plate (θ_w). In constructing the full system model, the flexibility of the spool plate must be incorporated as well; this is recognized when comparing the magnitudes of the plate deformation (see Table 4-2), washer deformation and total rotation of the CVT in Figure 5-5.



(a) Preload = 50% of flattening – elastic component is linear and given by equation (5-1)



(b) Preload = 25% of flattening – elastic component is S-shaped and given by equation (5-2)

Figure 5-4
Comparison on model and measured moment-rotation behavior when the model is driven by the measured θ_w as input (example shown for 2 units of 2U2D).

Summary of nonlinear dynamic model

Combining the moment-rotation model of equations (5-1) and (5-2) or (5-3) with the equation of motion of the CVT (considered as a rigid body), and including the flexibility of the spool plate results in the full nonlinear model of the Belleville washer-protected CVT:

$$\begin{aligned} \text{Equation of motion of CVT: } & (I_0 + ml^2)\ddot{\theta} + M_{CVT} = -ml\ddot{x}_g \\ \text{Hysteretic model (equation (5-3) rewritten): } & \dot{M}_{HYS} = k(1 - H_1 H_2)\dot{\theta}_w \end{aligned} \quad (5-4)$$

with $H_1 = \left| \frac{M_{HYS}}{M_{yield}} \right|^N$, $H_2 = (\eta + (1 - \eta) \operatorname{sgn}(M_{HYS}\dot{\theta}))$, M_{CVT} given by either equation (5-1) or (5-2), the spool plate deformation $\theta_p = \frac{M_{CVT}}{K_p}$ (K_p being the spool plate stiffness), $\theta_w = \theta - \theta_p$ and

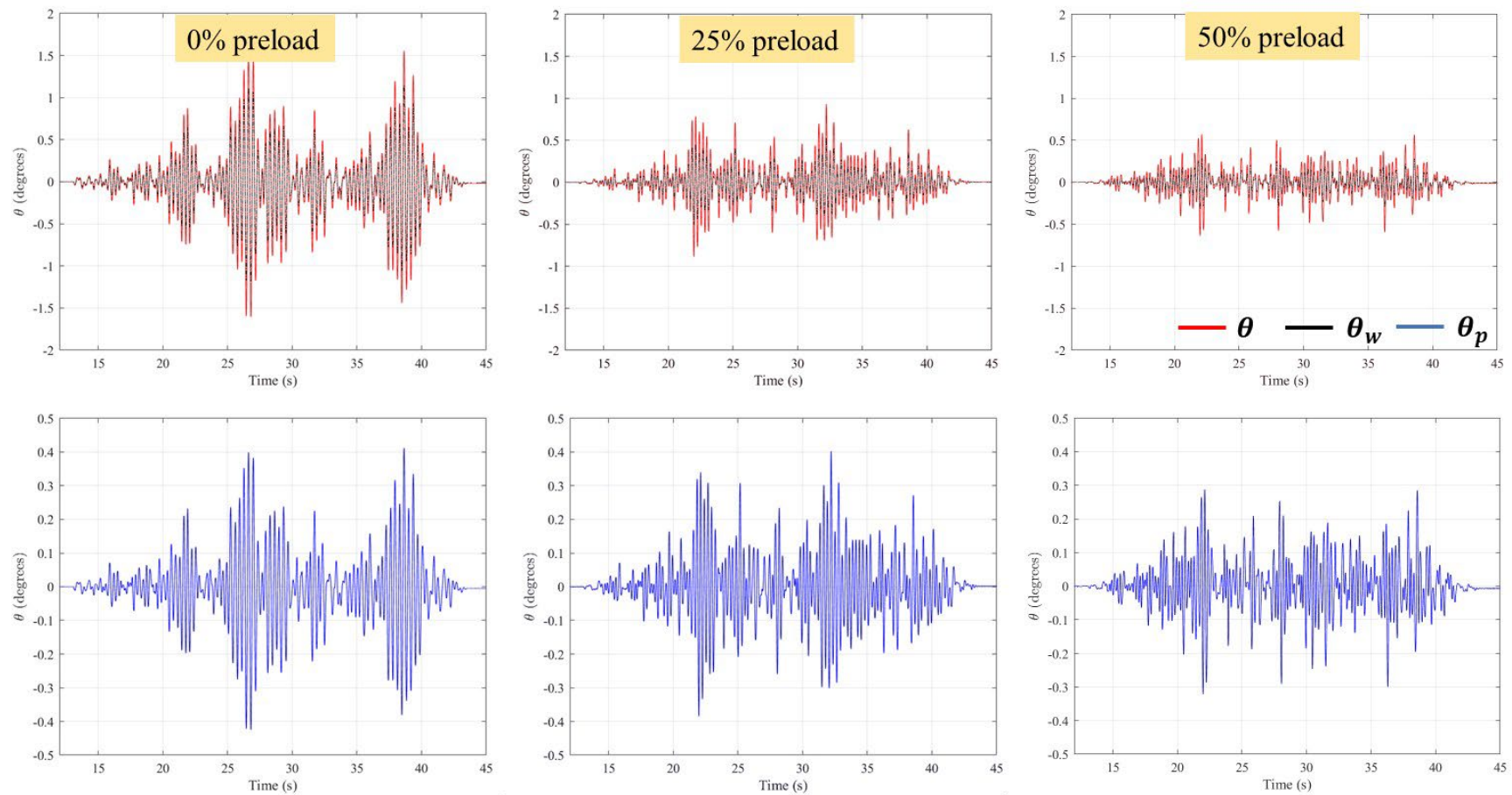


Figure 5-5

Relative magnitudes of total CVT rotation θ , washer stack deformation θ_w and spool plate deformation θ_p (example shown for 2 units of 2U2D in X direction for 0.5g CERL motion).

$\dot{\theta}_w = \left(\frac{K_p}{K_p + k(1 - H_1 H_2) + K} \right) \dot{\theta}$ for sufficient preload and $\dot{\theta}_w = \left(\frac{K_p}{K_p + k(1 - H_1 H_2) + K\alpha(1 - \tanh^2(\alpha\theta_w))} \right) \dot{\theta}$ for insufficient preload. Solutions to the differential equations (5-4) together with these auxiliary equations are computed using the solver `ode15s` in MATLAB [28]. The insulator moment can be calculated as an output of the analysis using equation (4-8).

Analysis results

As examples, analysis results are shown for 2 cases, but with the 2 units of 2U2D configuration under 0.5g CERL motion in the X direction, one case with 50% preload and another with 25% preload in Figure 5-6 and Figure 5-7.

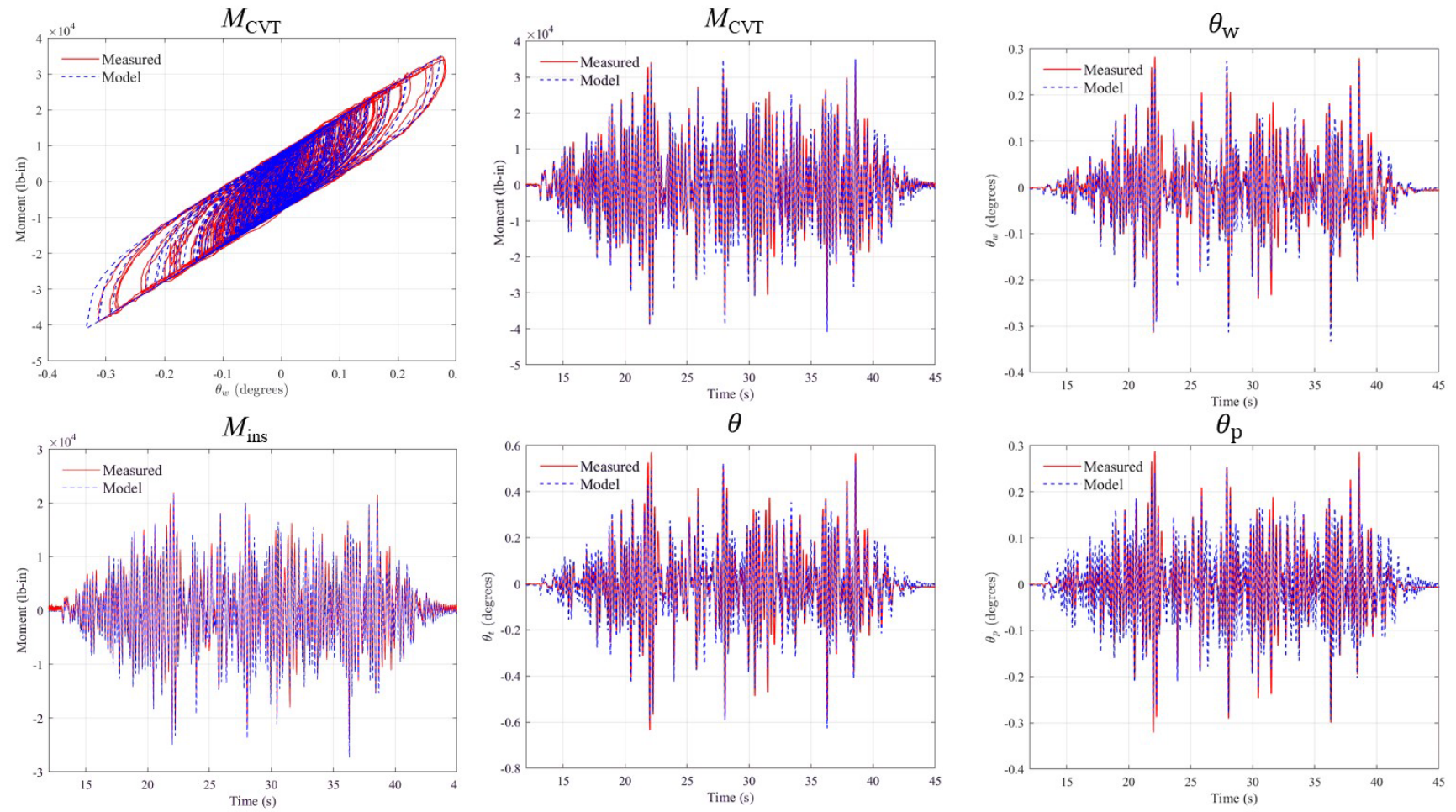


Figure 5-6

Various response quantities obtained from nonlinear dynamic analysis compared with corresponding measurements for 2 units of 2U2D in X direction for 0.5g CERL motion with 50% preload.

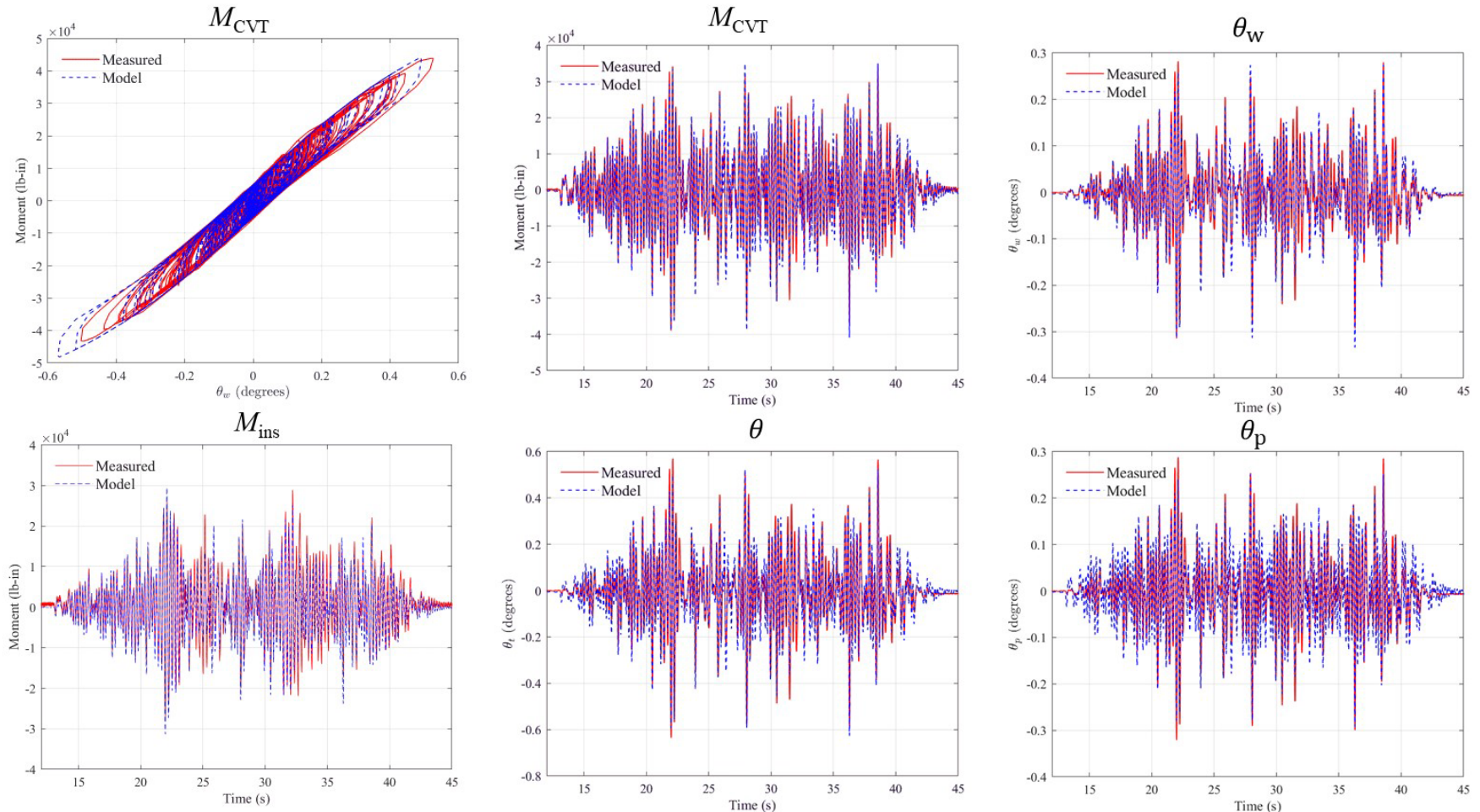


Figure 5-7

Various response quantities obtained from nonlinear dynamic analysis compared with corresponding measurements for 2 units of 2U2D in X direction for 0.5g CERL motion with 25% preload.

6

EQUIVALENT LINEAR MODELING

In the previous chapter, the Belleville washer-protected CVT system was analyzed using a nonlinear dynamic procedure. In this chapter, an alternate approach is presented using an equivalent linear approach. This approach may be better suited for practical use as well as provides insights in terms of system frequency and damping ratio. First, an equivalent linear model obtained by fitting to experimental measurements is presented; the frequencies and damping ratios so obtained are used as reference for the second approach. In the second approach, equivalent stiffnesses and damping ratios are obtained graphically from the moment-rotation hysteresis curves.

Identifying equivalent frequency and damping ratio from measurements

An equivalent linear model can be obtained from experimental measurements by fitting a linear model to it. Here, this is done using the subspace linear system identification method [29]. Figure 6-2 shows a comparison of such a linear fit with measured responses. Table 6-1 summarizes equivalent frequencies and damping ratios for all the configurations tested.

Graphical determination of equivalent stiffness and damping ratio

Approximate equivalent stiffness, frequency and damping ratio can be obtained graphically as illustrated in Figure 6-1. The equivalent stiffness, k_{eq} , is obtained as the ratio of the difference between the positive and negative peak moments and the difference between the peak positive and negative rotations. The frequency is then

$$f = \frac{1}{2\pi} \sqrt{\frac{k_{eq}}{I_0 + mh_{CG}^2}} \quad (6-1)$$

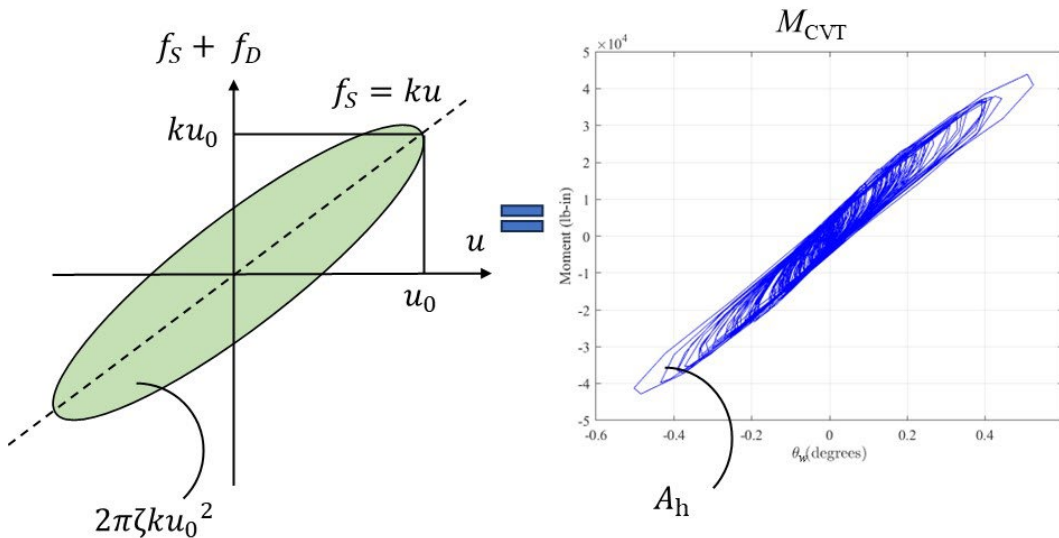


Figure 6-1
Concept of graphically obtaining equivalent stiffness and damping ratio.

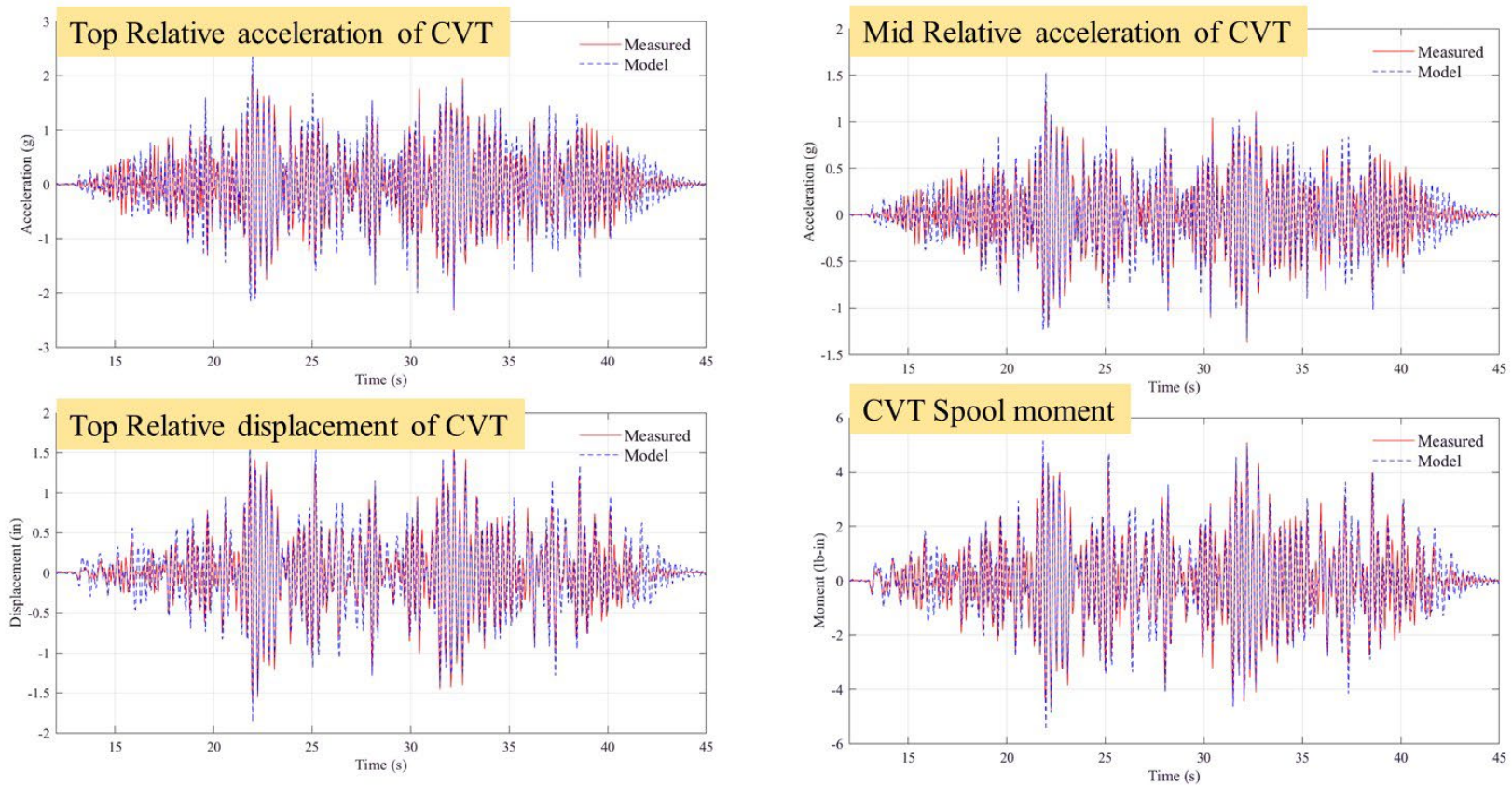


Figure 6-2

Comparison of measurements with linear fit obtained using subspace system identification for 0.5g CERL excitation in the X direction for 2 units of 2U2D configuration.

Table 6-1

Summary of findings from experimental measurements and equivalent linear modeling for 0.5g CERL excitation. Damping ratios in parentheses denote those obtained by the procedure in XXX.

Configuration	CVT fixed on spool (reference)		K1875-G-086 2 units of 2U2D						K1875-G-086 3 units of 3U3D			
Preload level	-		0%		25% (500lbs)		50% (1000lbs)		17% (500lbs)		50% (1500lbs)	
Direction of excitation	<i>X</i>	<i>Y</i>	<i>X</i>	<i>Y</i>	<i>X</i>	<i>Y</i>	<i>X</i>	<i>Y</i>	<i>X</i>	<i>Y</i>	<i>X</i>	<i>Y</i>
Natural frequency (Hz)	6.9	9.4	2.9	4.0	3.6	5.1	4.1	5.5	3.6	5.1	4.5	5.9
Damping ratio (%)	0.5	0.6	3.9	3.7	6.5	6.4	9.9	8.1	7.8	7.3	9.3	6.0
Maximum insulator base moment ($\times 10^4$ lb-in)	5.1	4.5	3.5	4.0	2.9	3.2	2.4	3.3	2.7	3.0	2.4	2.9
Maximum relative terminal displacement (in)	0.9	0.6	3.4	2.1	1.8	1.1	1.4	1.0	1.8	1.1	1.2	0.9

and the damping ratio is obtained by equating the area of the hysteresis, A_h , to that of a viscous damper undergoing the same peak displacement at steady state with frequency f [30]

$$\zeta = \frac{A_h}{2\pi k_{eq} u_0^2} \quad (6-2)$$

where These formulas parallel equations (17.2-4) and (17.2-4) of Chapter 17 of ASC 7-16 on Seismically Isolated Structures [31].

Response-spectrum interpretation

It can be seen from Table 6-1 that the insulator base moment is reduced in all configurations relative to the fixed base case, and by over 50% in the X direction and by over 25% in the Y direction for the cases with sufficient preload. This however comes at the expense of greater terminal displacement, about 50% greater for the cases with highest preload. These effects are similar to that of seismic isolation. These effects can be better understood by mapping the frequencies and damping ratios of the different configurations on a spectral plot as seen in Figure 6-2. For each configuration, the abscissa is the frequency and the ordinate is the spectral acceleration obtained from the equations in [32] for the damping ratio of that configuration.

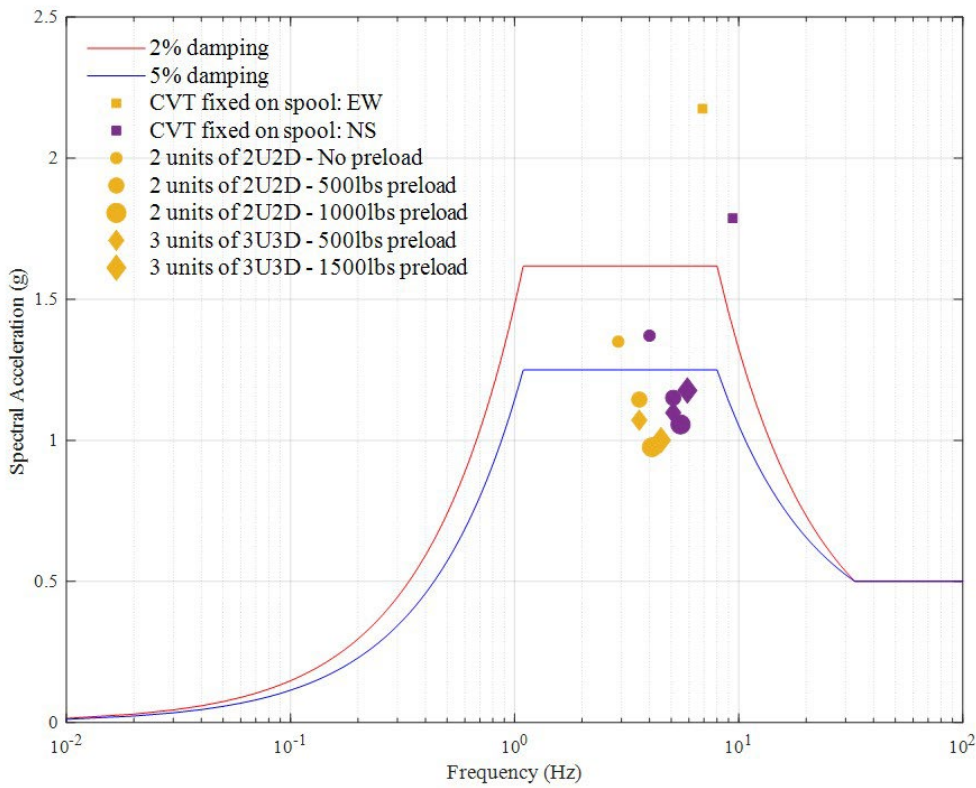


Figure 6-3
Frequencies and damping ratios corresponding to different Belleville washer configurations overplotted on the 2%- and 5%-damped required response spectrum (RRS) from IEEE 693-2018 [32].

The picture conveys the relative effectiveness of the different Belleville washer configurations with respect to the reference configuration. There is a frequency reduction that for the configurations tested does not play a major role in reducing base moments. The biggest effect is the increased damping. While such deductions can be made from the figure, the main takeaway is that with the tools developed in this project, a similar evaluation can be done for any other arrangement of washers by modeling and analysis. For example, a different configuration may be designed that further reduces frequency while increasing damping, trading off lower insulator base moment with increased terminal displacement.

7

SUMMARY AND CONCLUDING REMARKS

Executive summary

A modeling procedure has been developed to predict the seismic response of rigid equipment such as CVTs equipped with Belleville washer stacks at the base for seismic protection. The procedure allows for nonlinear dynamic analysis or an equivalent linear analysis, and is outlined in Chapter 2. The starting points are (a) the force-displacement hysteretic behavior of an individual stack that can be readily obtained by cyclic loading in a materials test machine, (b) inertia properties of the CVT – mass, mass moment of inertial and center of mass location. With this, the seismic response can be predicted reliably. This has been validated with experiments on an earthquake simulator (shake table). Special instrumentation was developed to obtain detailed in situ measurements of the behavior of the washer stacks in the shake table experiments. Validation using these measurements provides confidence that the analysis procedure can be used to inform decisions when installing Belleville washer devices in the field. The process also parallels procedures in ASCE 7-16 for seismic isolators.

The washer stacks essentially act as seismic isolators, reducing the frequency and increasing the damping. They are effective in reducing the insulator base moment. As is the case with seismic isolation systems, reduction is base moment has to be traded off with increase in terminal displacement.

Outstanding research questions

Some outstanding research questions remain:

Testing and modeling with different washer types; only one washer type has been studied completely (K1875-G-086). A second washer type has been studied partially (K1750-J-057), but some issues were discovered and are being remedied. It will be useful to complete the study with the K1750 washer type, as well as one other washer type from a different vendor.

Testing and modeling beyond flattening load: When subject to earthquake larger than what the spring washer protective system is designed for, the washer is likely to flatten, causing a different type of dynamics. It will be useful to study this performance under extreme loading. This is similar to when a base isolation system hits its displacement limit, which is considered in the design.

Testing and modeling single acting configuration: Thus far, we have only test cases with the spring washers in a single acting configuration, but that one configuration revealed promising behavior consisting of flag-shaped hysteretic behavior. It will be useful to study this further.

8

REFERENCES

1. Couch, R. and R. Deacon, *Procedures and criteria for increasing the earthquake resistance level of electrical substations and special installations*. 1973, Agbabian Associates, El Segundo, CA (USA).
2. Cochran, R., *Seismic Base Isolation of a High Voltage Transformer*, in *Electrical Transmission and Substation Structures 2015*. 2015. p. 413-425.
3. Kempner Jr., L. and M.J. Riley. *High voltage transformer base isolation*. in *Proceedings of the Canadian Association for Earthquake Engineering 2015*.
4. Oikonomou, K., et al., *Seismic isolation of high voltage electrical power transformers*, in *Techincal Report 2016*.
5. Saadeghvaziri, M.A., et al., *On Seismic Response of Substation Equipment and Application of Base Isolation to Transformers*. IEEE Transactions on Power Delivery, 2010. **25**(1): p. 177-186.
6. Blunt, N. *The Difference Between Disc Springs and Belleville Washers*. 2021.
7. Shigley, J.E. and C.R. Mischke, *Standard handbook of machine design*. 1996: McGraw-Hill.
8. Ashworth, G., *The Disk Spring or Belleville Washer*. Proceedings of the Institution of Mechanical Engineers, 1946. **155**(1): p. 93-100.
9. Almen, J.O. and A. Laszlo, *The uniform-section disk spring*. Transactions of the American society of mechanical engineers, 1936. **58**(4): p. 305-314.
10. Zhou, Y., et al., *Modeling of disc springs based on energy method considering asymmetric frictional boundary*. Thin-Walled Structures, 2023. **190**: p. 110971.
11. Korytov, M., et al. *Use of the Belleville spring package in the vibration protection mechanism of the operator's seat*. in *Journal of Physics: Conference Series*. 2022. IOP Publishing.
12. Maletta, C., L. Filice, and F. Furgiuele, *NiTi Belleville washers: Design, manufacturing and testing*. Journal of intelligent material systems and structures, 2013. **24**(6): p. 695-703.
13. Solon Manufacturing Co. *Belleville Spring Washer Applications & Solutions*. 2024; Available from: <https://www.solonmfg.com/washer-applications>.
14. Fujita, T., et al. *Fundamental study of three-dimensional seismic isolation system for nuclear power plants*. in *Proceedings, 11th world conference on earthquake engineering, Acapulco, Mexico*. 1996.
15. Kitamura, S., et al., *Experimental Study on Coned Disk Springs for Vertical Seismic Isolation System (K143)*. 2003.
16. Kitamura, S., S. Okamura, and K. Takahashi. *Experimental Study on Vertical Component Seismic Isolation System With Coned Disk Spring*. in *ASME 2005 Pressure Vessels and Piping Conference*. 2005.
17. Ramhormozian, S., et al., *Stiffness-based approach for Belleville springs use in friction sliding structural connections*. Journal of Constructional Steel Research, 2017. **138**: p. 340-356.
18. Speicher, M., et al., *Shape Memory Alloy Tension/Compression Device for Seismic Retrofit of Buildings*. Journal of Materials Engineering and Performance, 2009. **18**(5-6): p. 746-753.
19. Hill, K.E., *The utility of ring springs in seismic isolation systems*, in *Department of Mechanical Engineering*. 1995, University of Canterbury, Christchurch, New Zealand.
20. Ma, K., Y. Zhou, and D. Lu, *Theoretical and experimental investigation on disc spring isolation system with loading rings*. Soil Dynamics and Earthquake Engineering, 2023. **165**: p. 107655.
21. Institute of Electrical and Electronics Engineers, *IEEE Recommended Practices for Seismic Design of Substations Std 693-1984*. 1984. p. 1-13.
22. Key Bellevilles. *Belleville Products Sample Catalog*. 2024; Available from: <https://keybellevilles.com/bellevilles/sampleCatalog>.
23. Bouc, R. *Forced vibrations of mechanical systems with hysteresis*. in *Proc. of the Fourth Conference on Nonlinear Oscillations, Prague*, 1967. 1967.
24. Wen, Y.-K., *Method for random vibration of hysteretic systems*. Journal of the engineering mechanics division, 1976. **102**(2): p. 249-263.
25. Sivaselvan, M.V. and A.M. Reinhorn, *Hysteretic models for deteriorating inelastic structures*. Journal of engineering mechanics, 2000. **126**(6): p. 633-640.
26. Sivaselvan, M.V. and A.M. Reinhorn, *Nonlinear structural analysis towards collapse simulation: A dynamical systems approach*. 2004.
27. Constantinou, M.C. and M. Adnane, *Dynamics of Soil-base-isolated-structure Systems: Evaluation of Two Models for Yielding Systems. Report 4*. 1987: [Department of Civil Engineering], Drexel University.
28. The Mathworks Inc, *MATLAB version: 9.13.0 (R2022b)*. 2022, The MathWorks Inc.: Natick, Massachusetts, United States.
29. Van Overschee, P. and B. De Moor, *Subspace identification for linear systems: Theory—Implementation—Applications*. 2012: Springer Science & Business Media.

30. Chopra, A.K., *Dynamics of structures : theory and applications to earthquake engineering*. Sixth edition. ed. Prentice Hall international series in civil engineering and engineering mechanics. 2023, Hoboken, NJ: Pearson. pages cm.
31. American Society of Civil Engineers, *Minimum Design Loads and Associated Criteria for Buildings and Other Structures, ASCE 7-16*. 2017.
32. Institute of Electrical and Electronics Engineers, *IEEE Recommended Practice for Seismic Design of Substations Std 693-2018*. 2019.